

Optimising Principle for Non-Equilibrium Phase Transitions and Pattern Formation with Results for Heat Convection

Phil Attard

(Dated: 25 July, 2012. phil.attard1@gmail.com)

Spontaneous transitions between non-equilibrium patterns are characterised by hydrodynamic calculations of ideal straight roll steady state heat convection. The calculations are tested quantitatively against existing experimental data. It is shown that at a given Rayleigh number the final wave number depends upon whether the initial state was the conducting state, or, in the case of the cross roll transition, the wave number of the initial straight roll state. The final wave number does not correspond to the maximum or to the minimum heat flux (entropy production or dissipation), nor to the maximum sub-system entropy. In all cases the entropy of the total system increases monotonically during the spontaneous transition. It is concluded that there does not exist any single time thermodynamic property or variational principle for non-equilibrium systems. It is further concluded that the second entropy is *the* two time variational principle that determines the optimum non-equilibrium state or pattern.

I. INTRODUCTION

In the case of equilibrium systems, there is a well established variational principle for determining the optimum state, namely that the total entropy is a maximum, or, equivalently, that the free energy is a minimum. In the case of non-equilibrium systems, there is no such generally agreed principle, despite much effort and many claims. The two most common ideas invoke the rate of entropy production, with one school of thought claiming that it is a maximum, and another school of thought claiming that it is a minimum. The postulated ideas are mutually contradictory and there is a dearth of experimental or computational evidence to support either view.

In what remains of this introduction, and to foreshadow the numerical results for heat convection that are the main work of this paper, it is perhaps of historical and psychological interest to explore why the rate of entropy production continues to be championed as a non-equilibrium variational principle despite the acknowledged lack of predictive success of the approach. In the first place there is the implicit assumption that their *ought* to be an optimum non-equilibrium state. To question this assumption is not so bizarre as it might seem at first sight, as the numerical results obtained in this paper will show. The reason for uncritically assuming the existence of a non-equilibrium variation principle probably lies in the observation that in a given non-equilibrium system there are often quite distinct states or patterns that spontaneously occur, often reproducibly influenced by some control parameter. For example, in heat flow, there is the critical Rayleigh number at which the conduction-convection transition occurs, and for convection, there appear distinct steady state patterns (ideal straight rolls, hexagonal cells) of particular wave numbers, depending upon the boundary conditions, and other sometimes unidentified influences. The patterns that form in non-equilibrium systems can be quite spectacular, and it is natural to assume that the one selected by the system in a given case is the result of some general

thermodynamic principle.

This idea that there must exist a variational principle for non-equilibrium systems is also motivated by the success of the Second Law of Thermodynamics for equilibrium systems. The principle that the optimum equilibrium state is the state of maximum entropy has been demonstrably successful in accounting for the selection of competing equilibrium states. One can see how this might motivate many to think that there ought to exist an analogous variational principle for non-equilibrium systems. From this many workers simply extrapolate the Second Law of (Equilibrium) Thermodynamics to assert that, since in the time-independent case entropy is a maximum, in the time-dependent case it is the rate of production of entropy that must be a maximum. Whereas the Second Law of (Equilibrium) Thermodynamics was postulated by Clausius *after* much experimental observation and measurement, the principle that the rate of entropy production be maximised does not come from any observation, calculation, or measurement. What is more, Boltzmann's discovery of the molecular basis of entropy in terms of the number of configurations in a state provided a rational explanation, a physical interpretation, and mathematical framework for the Second Law. This again contrasts with the non-equilibrium case where there is a disconnect between the molecular picture of entropy and the assertion that the rate of entropy production is a maximum.

The historical origin of the opposite postulate, that the rate of entropy production is a minimum, appears to predate thermodynamics itself. As discussed by Jaynes in his review of the Principle of Minimum Entropy Production,¹ in 1848 Kirchhoff² developed certain theorems for electrical circuits, and showed that the electrical currents that flowed could be derived from a Principle of the Least Dissipation of Energy. Of course there is no question of the mathematical veracity of Kirchhoff's theorem for electrical circuits, but, as is discussed next, there is considerable reason to doubt the thermodynamic interpretation that they are equivalent to a Principle of Least Dissipation of Entropy and that such a principle

has general application for non-equilibrium systems.

In §II that follows this introduction, a detailed historical review and mathematical critique of these two conventional ideas for non-equilibrium systems is given. As well, comparison is briefly made with the author's own variational principle for non-equilibrium systems, namely that the second entropy is maximised. In §III, the hydrodynamic equations for convection are given, and in §IV expressions for the total first entropy of convection are derived. The computer algorithm is given in §V for the one dimensional case of ideal straight rolls, and in §VI the two dimensional case of the cross roll transition. In §VII, the convection calculations are compared with experimental measurements for spontaneous transitions, and various properties of heat convection are tested. In §VIII general conclusions are drawn from the numerical results for the optimising principle that gives the selected state of non-equilibrium systems.

II. CRITIQUE OF NON-EQUILIBRIUM VARIATIONAL PRINCIPLES

In this section three non-equilibrium variational principles, —Minimum Dissipation, Maximum Dissipation, and Second Entropy— are presented in their simplest forms in order to compare their strengths and weaknesses, and the evidence for and against each one.

A. Principle of Minimum Dissipation

1. Kirchhoff's Version

Onsager,⁴ in his celebrated paper on the reciprocal relations, gave two different Principles of Minimum Dissipation. The first is directly related to Kirchhoff's Principle of Least Energy Dissipation and is treated here. The second is related to the vanishing of fluxes conjugate to quiescent variables and is discussed in the following subsection.

In 1848 Kirchhoff generalised Ohm's law to three dimensions and noted that the current in any region was determined by minimising the energy dissipation (Joule heating) with respect to the voltage for specified values on the surface.² This principle of least energy dissipation was derived by Kirchhoff from the fact that in the steady state electrical charge could not accumulate at any point.

For the present purposes, and following Jaynes,¹ it is sufficient to consider two resistors, R_1 and R_2 connected in parallel with total current $J = J_1 + J_2$ flowing through them. (The total current is equivalent to a potential drop of $\phi = J[R_1^{-1} + R_2^{-1}]^{-1}$.) The energy dissipation or Joule heat is

$$\dot{E} = J_1^2 R_1 + J_2^2 R_2 = J_1^2 R_1 + [J - J_1]^2 R_2. \quad (2.1)$$

The derivative of this at constant total current (equiva-

lently, fixed potential drop) is

$$\frac{\partial \dot{E}}{\partial J_1} = 2J_1 R_1 - 2[J - J_1]R_2, \quad (2.2)$$

which vanishes when

$$\bar{J}_1 = \frac{R_2}{R_1 + R_2} J. \quad (2.3)$$

This current minimises the energy dissipation and is of course just the current that one would obtain directly from Ohm's law.

The Principle of Least Entropy Dissipation appears to follow from this by considering the case that the resistors are in thermal contact with a reservoir of temperature T , so that the rate of production of entropy in the reservoir is just $\dot{S}_r = \dot{E}/T$. Hence minimising the energy dissipation is the same as minimising the entropy dissipation.

There are two major problems with the extrapolation of Kirchhoff's principle of electrical circuits to a general principle for non-equilibrium systems. First, the principle of least dissipation of energy has nothing to do with entropy. To see this simply consider the case that the resistors are in contact with two separate reservoirs of temperature T_1 and T_2 respectively. The currents do not change, but the entropy production is no longer a minimum. (The minimum entropy dissipation would occur when $\bar{J}_1 = R_2 J / T_2 [(R_1/T_1) + (R_2/T_2)]$, which obviously violates Ohm's law.)

The first problem also signifies a common misunderstanding of non-equilibrium variational principles, namely it is often not precisely clear what one is trying to achieve by such a principle. In the present problem of current flow, Ohm's law already completely specifies the current flow for the stated problem. There is no point in formulating a variational function for current flow unless it has application beyond Ohm's law. More generally, any non-equilibrium variational principle has to be explicitly formulated as consistent with, but providing something beyond, the linear transport laws. This point will be further discussed below.

The second problem with the thermodynamic interpretation is that only part of the entropy dissipation has been considered. The battery or source of electromotive force that drives the current also dissipates entropy. If the state of non-equilibrium systems were truly determined by the entropy dissipation, then surely it is the total entropy dissipation that is relevant.

On this point it is worth mentioning the work of Županović et al.,³ also based on Kirchhoff's laws, but in this case giving a Principle of *Maximum* Entropy Dissipation. The reason that they obtained a maximum rather than the more traditional minimum is that they took into account the energy supplied by the electromotive forces and invoked energy conservation as a constraint on the variation of the Joule heat. But their thermodynamic conclusion is vitiated for the same reason as just discussed, namely that the result comes directly from

Ohm's law (and energy conservation) and has nothing to do with entropy. If the resistors in the circuit are at different temperatures, and if the entropy dissipated by the batteries and sources of electromotive force is taken into account, then the entropy dissipation would no longer be maximal.

Onsager, in the first of his two celebrated papers on the reciprocal relations,^{4,5} gives a non-equilibrium variational principle, Eq. (6.6) of Ref. 4, which case he says has been named the 'Principle of the Least Dissipation of Energy'. Onsager says that if the boundary fluxes are specified, and if the sub-system is in a steady state, then Rayleigh's dissipation function, a quadratic of the fluxes, is a minimum. Rayleigh's dissipation function has the same appearance as the Joule heat in Kirchhoff's Principle of Least Dissipation of Energy. Four criticisms can be made of Onsager's proposal, all of which can be made of any thermodynamic interpretation of Kirchhoff's Principle: First, that Rayleigh's dissipation function does not give the actual entropy dissipation for the arbitrary fluxes that are explored in the variational procedure. Second, that the rate of total entropy production is not accounted for. Third, since one can multiply Rayleigh's dissipation function by an arbitrary constant, including a negative one, and still obtain the same optimum value, the variational function cannot be a physical thermodynamic potential. Fourth, and connected with the third, the variational procedure yields nothing beyond the built-in linear transport laws, not even the reciprocal relations.

2. Onsager's Version

Onsager gives a second form of the Principle of Minimum Entropy Dissipation (Principle of Least Dissipation, for short) in § 6 of Ref. 4, leading up to and following his Eq. (6.5). This version of the Principle is said to apply to certain non-equilibrium systems when some of the fluxes vanish. Identical Principles of Minimum Entropy Dissipation for vanishing fluxes have been invoked by Prigogine,⁶ and by de Groot and Mazur.⁷

Onsager claims that this Principle gives rise to the reciprocal relations (see p. 424 of Ref. 4). He dwells upon the historical antecedents of the Principle (he attributes it to Helmholtz and to Kelvin rather than to Kirchhoff) in his acceptance speech for the Nobel prize.⁸ The claim that it is the basis of the reciprocal relations is also made by Mazur in his summary of Onsager's achievements.⁹ If true, such a result would provide a distinct derivation of the reciprocal relations that was independent of the microscopic reversibility derivation that Onsager actually used, and it would arguably justify regarding this particular Principle of Minimum Entropy Dissipation as a fundamental thermodynamic principle. This claim will now be tested.

For simplicity consider an isolated system, with $\mathbf{x} \equiv \{x_1, x_2, \dots, x_n\}$ being the non-conserved material quantities of interest. The associated fluxes are $\mathbf{J} \equiv$

$\{J_1, J_2, \dots, J_n\}$ with $J_i \equiv \dot{x}_i^0/V$, the superscript zero signifying an isolated system. The conjugate thermodynamic forces, $\mathbf{X} \equiv \{X_1, X_2, \dots, X_n\}$, are the derivatives of the entropy, $X_i \equiv \partial S(\mathbf{x})/\partial x_i$. For example, the relevant extensive material variable might be the first energy moment, in which case the thermodynamic force is the reciprocal of the first temperature, which is essentially the temperature gradient, and the flux is the energy crossing a plane per unit area per unit time.

The specified structure \mathbf{x} , or equivalently force $\mathbf{X}(\mathbf{x})$, is considered to have arisen as a fluctuation from the equilibrium state of the isolated system, and the flux \mathbf{J} represents the regression of the fluctuation back to the equilibrium state.

It will turn out that the analysis is equivalent to examining the coupling between forces and fluxes in the case that some of the variables are relevant variables, and others are quiescent variables. Relevant or active variables have a specified value of the thermodynamic force (equivalently the value of the material property), that results either from a fluctuation of an isolated system or else from exchange with reservoirs. Quiescent or slave variables have either zero force (in the instant of the initial fluctuation of the active variable for an isolated system), or zero flux, (for a steady state sub-system with the quiescent variables being non-exchangeable with the reservoir).

For example, in the case of thermodiffusion, one has two material properties, namely the moments of energy and number. If one wants to concentrate on heat flow, then one can still use the two component formalism, but treat the number variables as quiescent and set their fluxes to zero (and one can calculate the non-zero value of the thermodynamic force on the number). Alternatively, and ultimately equivalently, one can consider a single component of energy alone, and never consider explicitly the number fluxes or forces. In the full case when both are active, the energy and mass fluctuations are non-zero, and their fluxes are both non-zero.

There are two questions: First, do the reciprocal relations imply the Principle of Least Dissipation (with respect to the quiescent fluxes)? Second, does the Principle of Least Dissipation imply the reciprocal relations?

For simplicity consider everything to be uniform in space. By definition, the rate of entropy production per unit volume of the system is

$$\dot{S}/V \equiv \mathbf{J} \cdot \mathbf{X}. \quad (2.4)$$

This exact formula holds whether or not the fluxes are the optimal ones. This will be called the dissipation.

The phenomenological or linear transport laws say that the fluxes are proportional to the thermodynamic forces,

$$\mathbf{J} = \underline{\underline{A}}\mathbf{X}. \quad (2.5)$$

In this form of the linear transport laws, the n forces are regarded as the independent variables.

Here Onsager's notation for the fluxes is used rather than the present author's. The present author always distinguishes between arbitrary fluxes \mathbf{J} and optimal fluxes $\bar{\mathbf{J}}$; only the latter obey the linear transport laws. Onsager (and most other authors) do not distinguish the two explicitly. Because one is carrying out variational procedures for arbitrary fluxes, it can be difficult to figure out precisely which equations assume the linear transport laws and which do not.

With the linear transport laws in this form with the forces as independent variables, the dissipation becomes a quadratic form,

$$\dot{S}/V = \mathbf{X} \cdot \underline{\underline{A}} \mathbf{X}. \quad (2.6)$$

Since the Second Law of Thermodynamics mandates that the dissipation be positive, this implies that the transport matrix must be positive definite.

The Onsager reciprocal relations says that the transport matrix is symmetric,

$$\underline{\underline{A}} = \underline{\underline{A}}^T. \quad (2.7)$$

To answer the first question this will be assumed true. To answer the second question it will be checked whether or not the Principle of Least Dissipation implies this result.

Now the first m variables will be considered active, and the second $n - m$ will be considered quiescent. Use a sub-script 1 for the first m variables and 2 for the second $n - m$ variables, so that $\mathbf{J}_1 \equiv \{J_1, J_2, \dots, J_m\}$ and $\mathbf{J}_2 \equiv \{J_{m+1}, J_{m+2}, \dots, J_n\}$, and similarly for \mathbf{X}_1 and \mathbf{X}_2 . The transport matrix $\underline{\underline{A}}$ similarly breaks into four blocks, and the reciprocal relations imply

$$\underline{\underline{A}}_{11} = \underline{\underline{A}}_{11}^T, \underline{\underline{A}}_{22} = \underline{\underline{A}}_{22}^T, \text{ and } \underline{\underline{A}}_{12} = \underline{\underline{A}}_{21}^T. \quad (2.8)$$

In block form, the linear transport laws are explicitly

$$\begin{aligned} \mathbf{J}_1 &= \underline{\underline{A}}_{11} \mathbf{X}_1 + \underline{\underline{A}}_{12} \mathbf{X}_2 \\ \mathbf{J}_2 &= \underline{\underline{A}}_{21} \mathbf{X}_1 + \underline{\underline{A}}_{22} \mathbf{X}_2. \end{aligned} \quad (2.9)$$

Choosing the first m forces and the second $n - m$ fluxes as the independent variables, the linear transport laws may be rewritten

$$\begin{aligned} \mathbf{J}_1 &= \left[\underline{\underline{A}}_{11} - \underline{\underline{A}}_{12} \underline{\underline{A}}_{22}^{-1} \underline{\underline{A}}_{21} \right] \mathbf{X}_1 + \underline{\underline{A}}_{12} \underline{\underline{A}}_{22}^{-1} \mathbf{J}_2 \\ \mathbf{X}_2 &= -\underline{\underline{A}}_{22}^{-1} \underline{\underline{A}}_{21} \mathbf{X}_1 + \underline{\underline{A}}_{22}^{-1} \mathbf{J}_2. \end{aligned} \quad (2.10)$$

The rate of entropy production is a quadratic form in these independent variables

$$\begin{aligned} \dot{S}/V &= \mathbf{J}_1 \cdot \mathbf{X}_1 + \mathbf{J}_2 \cdot \mathbf{X}_2 \\ &= \mathbf{X}_1 \cdot \left[\underline{\underline{A}}_{11} - \underline{\underline{A}}_{12} \underline{\underline{A}}_{22}^{-1} \underline{\underline{A}}_{21} \right] \mathbf{X}_1 + \mathbf{X}_1 \cdot \underline{\underline{A}}_{12} \underline{\underline{A}}_{22}^{-1} \mathbf{J}_2 \\ &\quad - \mathbf{J}_2 \cdot \underline{\underline{A}}_{22}^{-1} \underline{\underline{A}}_{21} \mathbf{X}_1 + \mathbf{J}_2 \cdot \underline{\underline{A}}_{22}^{-1} \mathbf{J}_2 \\ &= \mathbf{X}_1 \cdot \underline{\underline{A}}^{(m)} \mathbf{X}_1 + \mathbf{J}_2 \cdot \underline{\underline{A}}_{22}^{-1} \mathbf{J}_2 \\ &\quad + \mathbf{J}_2 \cdot \left[(\underline{\underline{A}}_{22}^{-1})^T \underline{\underline{A}}_{12}^T - \underline{\underline{A}}_{22}^{-1} \underline{\underline{A}}_{21} \right] \mathbf{X}_1. \end{aligned} \quad (2.11)$$

Here $\underline{\underline{A}}^{(m)} \equiv \underline{\underline{A}}_{11} - \underline{\underline{A}}_{12} \underline{\underline{A}}_{22}^{-1} \underline{\underline{A}}_{21}$ is the $m \times m$ transport matrix that would hold if the active components only were considered. In this case the linear transport laws are $\mathbf{J}_1 = \underline{\underline{A}}^{(m)} \mathbf{X}_1$, as will now be shown.

Now if the reciprocal relations hold, then Eq. (2.8) implies

$$(\underline{\underline{A}}_{22}^{-1})^T \underline{\underline{A}}_{12}^T = \underline{\underline{A}}_{22}^{-1} \underline{\underline{A}}_{21}. \quad (2.12)$$

Hence the cross term vanishes and the dissipation becomes

$$\dot{S}/V = \mathbf{X}_1 \cdot \underline{\underline{A}}^{(m)} \mathbf{X}_1 + \mathbf{J}_2 \cdot \underline{\underline{A}}_{22}^{-1} \mathbf{J}_2. \quad (2.13)$$

Because the full transport matrix is positive definite, each of the two transport matrices that appear here must also be positive definite due to the combination of sub-blocks from which they are formed. Hence one can see that the reciprocal relations imply that the dissipation is minimised by the vanishing of the quiescent fluxes

$$\left. \frac{\partial \dot{S}/V}{\partial \mathbf{J}_2} \right|_{\mathbf{J}_2=0} = \mathbf{0}. \quad (2.14)$$

In this case, because $\mathbf{J}_2 = \mathbf{0}$, the linear transport laws, Eq. (2.10), become $\mathbf{J}_1 = \underline{\underline{A}}^{(m)} \mathbf{X}_1$, which are those that would apply if only the active components were considered.

This result proves that if the reciprocal relations hold, then the entropy dissipation is minimised by the vanishing of the quiescent fluxes. The significance or otherwise of this result will be discussed shortly.

Now to the second question: does minimising the dissipation with respect to the quiescent fluxes imply the reciprocal relations? Differentiating with respect to the independent fluxes the form of the dissipation that does not assume the reciprocal relations, Eq. (2.11), one obtains

$$\frac{\partial \dot{S}/V}{\partial \mathbf{J}_2} = \left[(\underline{\underline{A}}_{22}^{-1})^T \underline{\underline{A}}_{12}^T - \underline{\underline{A}}_{22}^{-1} \underline{\underline{A}}_{21} \right] \mathbf{X}_1 + 2 \underline{\underline{A}}_{22}^{-1} \mathbf{J}_2. \quad (2.15)$$

Demanding this vanish at $\mathbf{J}_2 = \mathbf{0}$ yields Eq. (2.12),

$$(\underline{\underline{A}}_{22}^{-1})^T \underline{\underline{A}}_{12}^T = \underline{\underline{A}}_{22}^{-1} \underline{\underline{A}}_{21}.$$

But this equation does not in general imply the block form of the reciprocal relations, Eq. (2.8), since the matrices cannot be separately equated.

For the case $n = 2$ and $m = 1$ these matrices are scalars. In this case, and only in this case, the scalar A_{22} cancels both sides and one is left with the scalar equality $A_{12} = A_{21}$, which is the reciprocal relation for two coupled flows. It is to be noted that both Onsager (see the discussion following Eq. (6.5) of Ref. 4), and Mazur (see the equations and discussion leading to Eq. (7) of Ref. 9), in claiming that the Principle of Least Dissipation implies the reciprocal relations, both offer only an $n = 2, m = 1$ example. One cannot deduce the properties of the matrix $\underline{\underline{A}}$ for general n from the pairwise

results obtained for $n = 2$ without making the additional assumption that the individual elements do not depend upon the other components of the system, which in any case appears to be false. For example, it is not true that the Soret coefficient for thermodiffusion does not depend on the specific solvent or on the concentrations of the other solutes. Whereas the reciprocal relations imply $A_{ij}^{(n)} = A_{ji}^{(n)}$, the extrapolation of the pairwise result would require $A_{ij}^{(n)} = A_{ji}^{(n')}$, which is not true in general.

In contrast, the reciprocal relations hold for an arbitrary number of active and quiescent variables; Eq. (2.8) contains more information than Eq. (2.12). One concludes that the reciprocal relations are sufficient but not necessary to ensure that the dissipation is minimised when the quiescent fluxes vanish. The present author cannot agree with the claim by Onsager⁴ and by Mazur⁹ that the Principle of Least Dissipation for quiescent fluxes implies the reciprocal relations.

Finally then, what actually is the use of the Principle of Minimum Dissipation? Is it really so surprising or significant that the entropy dissipation is reduced by setting some of the fluxes to zero, Eq. (2.13)? Is it even true that in the actual physical problem—the regression of a fluctuation of an isolated system—the flux of quiescent variables vanishes? In fact, at the first instant $\tau = 0$ of a fluctuation in the active variables, the force and flux of the quiescent variables is zero. At some intermediate time after that, the quiescent force is non-zero, and so the quiescent flux also must have been non-zero leading up to that state, and it must be non-zero going forward in time as both active and quiescent forces relax back to zero. (This is different to the steady state situation for a sub-system that can exchange with reservoirs, in which case the active and quiescent forces are constant in time, and the quiescent flux is zero.) One can conclude that whilst the reciprocal relations imply that the dissipation is minimised when the quiescent fluxes vanish, in many cases in the real world the quiescent fluxes do not vanish and the dissipation is not a minimum with respect to them.

More generally, the Principle of Minimum Dissipation does not give either the values of the active fluxes or the quiescent forces, since these come from the linear transport laws for the given active forces and the zero quiescent fluxes, Eq. (2.9). It is difficult to identify anything of import that is achieved by minimising the dissipation with respect to the quiescent fluxes, or to see how one might erect a full thermodynamic theory for non-equilibrium systems on this Principle.

B. Principle of Maximum Dissipation

Although most who assert the Principle of Maximum Dissipation do so based on nothing more than an analogy with the Second Law of Equilibrium Thermodynamics, Onsager actually attempted a detailed justification.

Onsager believed that a particular function that he formulated, the entropy dissipation less Rayleigh's dissipation function, was a thermodynamic potential for non-equilibrium systems. In fact, he asserted that 'the reciprocal relations... can be expressed in terms of a potential, and permit the formulation of a variational principle', (just prior to Eq. (5.1) of Ref.4).

Onsager, in Eq. (5.3) of Ref. 4, defined what will be called here the Rayleigh dissipation function,

$$\phi(\mathbf{J}) \equiv \frac{\alpha}{2} \mathbf{J} \cdot \underline{\underline{A}}^{-1} \mathbf{J}. \quad (2.16)$$

This is written in the present notation, with the constant α being introduced here in order to make a point about the arbitrariness of Onsager's functional; Onsager implicitly chooses $\alpha = 1$. Onsager says that this dissipation function was originally introduced by Rayleigh as a potential for frictional forces.¹⁰

As mentioned above, there is a certain ambiguity in Onsager's work regarding whether he regards the fluxes as arbitrary, as here and in his Eq. (5.3),⁴ or whether he restricts them to satisfying the linear transport laws, which he does in the second expression that he gives for the Rayleigh dissipation function, Eq. (5.5).⁴

This ambiguity underscores a significant problem with Onsager's work, namely that the Rayleigh dissipation function is only related to the entropy dissipation (it is equal to $\alpha/2$ times the entropy dissipation) when the fluxes are equal to the values given by the linear transport laws. For arbitrary fluxes, this function is not directly related to the entropy dissipation. Since Onsager is developing a variational principle for arbitrary fluxes, which he believes has the physical meaning of the non-equilibrium thermodynamic potential, it is crucial to appreciate that Rayleigh's dissipation function does not have the physical interpretation given it by Onsager.

Onsager, in Eq. (5.9) of Ref. 4, shows that the rate of total entropy production per unit volume, (here assuming spatial homogeneity), is

$$\dot{S}/V = \mathbf{J} \cdot \mathbf{X},$$

which was given above as Eq. (2.4). Although Onsager derived this for the general case of a sub-system and a reservoir, it also holds for the total isolated system considered here.

Onsager gives his variational functional as

$$\begin{aligned} \mathcal{O}(\mathbf{J}|\mathbf{X}) &\equiv \frac{\alpha \dot{S}}{V} - \phi(\mathbf{J}) \\ &= \alpha \mathbf{J} \cdot \mathbf{X} - \frac{\alpha}{2} \mathbf{J} \cdot \underline{\underline{A}}^{-1} \mathbf{J}, \end{aligned} \quad (2.17)$$

where again the α has been inserted here, since Onsager actually took $\alpha = 1$. It was of course necessary for Onsager to subtract the quadratic dissipation function $\phi(\mathbf{J})$ from the actual entropy dissipation because \dot{S} is linear in the flux and does not have an extremum. (A common feature of all the variational principles is that they

must contain a term quadratic in the fluxes and a term linear in the fluxes, with the latter being proportional to the entropy dissipation.) Onsager says that his function $\mathcal{O}(\mathbf{J}|\mathbf{X})$ is to be maximised over the fluxes for specified forces, (since the dissipation must be positive, \underline{A} must be positive definite, and the extremum has to be a maximum).

Onsager offers no particular physical justification for this choice of functional other than that it is optimised by the linear transport laws,

$$\bar{\mathbf{J}} = \underline{A}\mathbf{X}. \quad (2.18)$$

The maximum value of the variational functional is

$$\mathcal{O}(\bar{\mathbf{J}}|\mathbf{X}) = \phi(\bar{\mathbf{J}}) = \frac{\alpha}{2}\bar{\mathbf{J}} \cdot \mathbf{X}. \quad (2.19)$$

The right hand side is just $\alpha/2$ times the rate of entropy dissipation in the optimal state.

The linear transport laws emerge irrespective of the value of α . Onsager's analysis is equivalent to choosing a value of $\alpha = 1$. The physical basis for implicitly choosing $\alpha = 1$ is unstated by Onsager, but the consequence is that it is the entropy dissipation itself (less the Rayleigh dissipation function) that is maximised rather than some multiple thereof. As such, this has the appearance of being a physical quantity. Of course as a matter of logic Onsager could equally have chosen $\alpha = -1$, in which case he would have had a Principle of Minimum Dissipation. Perhaps Onsager, like other proponents of the Principle of Maximum Dissipation, implicitly chose $\alpha = 1$ by analogy with the Second Law of Equilibrium Thermodynamics.

Onsager's variational function upon which he based his Principle of Maximum Dissipation will next be compared with Attard's second entropy function,^{11,12} which amongst other things gives a particular value and physical interpretation to the quantity α . The point that can be made here is the arbitrary nature of Onsager's functional. As such it cannot be the non-equilibrium thermodynamic potential, because any ambiguity in such a potential would have measurable physical consequences. Onsager's implicit choice, $\alpha = 1$, corresponds to maximising the entropy dissipation, is no more justified than the choice $\alpha = -1$, which would correspond to minimising the entropy dissipation; both choices are in fact incorrect, as will now be shown. Finally, despite the assertion made by Onsager and quoted above, no evidence is offered by him that the variational function is necessary for the reciprocal relations. (By design, the variational functional is sufficient to yield the linear transport laws.)

A variety of variational principles can be constructed from different combinations of the quadratic dissipation functions $\dot{S}(\mathbf{J}, \mathbf{X}) \equiv \mathbf{J} \cdot \mathbf{X}$, $\phi(\mathbf{J}) \equiv \mathbf{J} \cdot \underline{A}^{-1}\mathbf{J}/2$, and $\psi(\mathbf{X}) \equiv \mathbf{X} \cdot \underline{A}\mathbf{X}/2$. These have featured in a number of postulated thermodynamic potentials for non-equilibrium systems in the literature, as has been reviewed by the present author.¹³ By design these always give the linear transport laws as their optimum state, but

they are subject to the same criticisms as have been made above: In general the functions have no physical meaning away from the optimum state, and so they don't provide the actual driving force toward the optimum state. Also, there is no physical basis for extremising the dissipation, and therefore there is no fundamental thermodynamic justification for the postulated functions.

C. The Second Entropy

The present author gave a variational principle for the fluxes and structure based upon the so-called second entropy, which can also be called the transition entropy, or the two-time entropy. The full theory is given elsewhere.^{11,12} Here it suffices to say that the theory treats as the fundamental non-equilibrium object the transition between two states in a specified time interval, $\mathbf{x} \xrightarrow{\tau} \mathbf{x}'$. The flux is essentially defined as the coarse derivative, $\mathbf{J} \equiv [\mathbf{x}' - \mathbf{x}]/\tau V$. In fluctuation form, the first (or ordinary, or structural) entropy is

$$S^{(1)}(\mathbf{x}) = \frac{1}{2}\mathbf{x} \cdot \underline{S}\mathbf{x}, \quad (2.20)$$

the thermodynamic force is $\mathbf{X} = \underline{S}\mathbf{x}$, and the second entropy is, (in the present notation),

$$\begin{aligned} \frac{S^{(2)}(\mathbf{J}, \mathbf{x})}{V} = & \frac{-|\tau|}{4}\mathbf{J} \cdot \underline{A}^{-1}\mathbf{J} + \frac{\tau}{2}\mathbf{J} \cdot \mathbf{X} \\ & + \frac{|\tau| - 2\tau}{4}\mathbf{X} \cdot \underline{A}\mathbf{X} + \frac{S^{(1)}(\mathbf{x})}{V}. \end{aligned} \quad (2.21)$$

This holds for arbitrary fluxes that do not necessarily obey the linear transport laws. The all-important coefficient of the cross term, which makes it half the dissipation, as well as the final two terms, which are constant with respect to the fluxes and which are therefore of lesser importance, come from a small time expansion and the so-called reduction condition,

$$S^{(2)}(\bar{\mathbf{J}}, \mathbf{x}) = S^{(1)}(\mathbf{x}). \quad (2.22)$$

This is formally exact and is simply a statement of Boltzmann's molecular definition of entropy.^{11,12}

It is evident that the second entropy is maximised with respect to the fluxes when the linear transport laws are satisfied,

$$\left. \frac{\partial S^{(2)}(\mathbf{J}, \mathbf{x})}{\partial \mathbf{J}} \right|_{\mathbf{J}=\bar{\mathbf{J}}} = \mathbf{0} \Leftrightarrow \bar{\mathbf{J}} = \underline{A}\mathbf{X}, \quad (2.23)$$

going forward in time, $\tau > 0$. Hence maximising the second entropy is equivalent to the linear transport laws. But the second entropy itself is valid for non-optimal fluxes that do not satisfy the linear transport laws.

From the nature of the derivation of the second entropy, specifically that the fluctuations in an equilibrium system are time symmetric, the coefficient matrix is symmetric, $\underline{A} = \underline{A}^T$ (at least for variables of pure time parity). Hence the second entropy implies the Onsager reciprocal relations.

1. Comparison with Onsager's First Function

Comparing Onsager's variational function Eq. (2.17) with Attard's second entropy, Eq. (2.21) going forward in time, $\tau > 0$, one sees that apart from the immaterial terms that are constant with respect to the fluxes, the two are proportional to each other

$$\mathcal{O}(\mathbf{J}|\mathbf{X}) = \frac{2\alpha}{\tau} S^{(2)}(\mathbf{J}, \mathbf{X}) + \text{const.} \quad (2.24)$$

This says that the physically correct value is $\alpha = \tau/2$ (at least going forward in time). As mentioned above, any variational principle for the non-equilibrium thermodynamic potential must be a quadratic in the fluxes, and so the only choice in the functional form is for the three coefficients of the quadratic equation. Since only differences in potentials have physical meaning, any constant term is immaterial, and so there are two coefficients to determine. One coefficient is fixed by demanding that the optimum flux satisfy the linear transport laws. The remaining degree of freedom was fixed by Onsager by demanding that it be the rate of entropy dissipation itself that be maximised, $\alpha = 1$. There is no physical requirement for this. In Attard's second entropy case, this remaining degree of freedom was instead fixed by the formally exact requirement that the second entropy reduce to the first entropy in the optimum state. (The analysis was actually a little more complicated than this in that it required a small time expansion of the fluctuation matrices, equating the coefficients term by term in the reduction condition.)^{11,12}

As mentioned above, the arbitrary nature of the justification for Onsager's functional actually has physical consequences that preclude it from being a proper thermodynamic potential. Onsager's implicit choice of $\alpha = 1$ means that his function $\mathcal{O}(\mathbf{J}|\mathbf{X})$ and the second entropy $S^{(2)}(\mathbf{J}, \mathbf{X})$ have different curvatures. If the functionals are to represent the non-equilibrium thermodynamic potential, then their exponential must give the probability distribution of the fluxes, and their curvature must give the fluctuations in the fluxes. Because the second entropy is the physical entropy, it gives the probability of a fluctuation in fluxes and structure in an equilibrium system. The arbitrary choice $\alpha = 1$ by Onsager yields incorrect fluctuations in the fluxes.

2. Comparison with Onsager's Second Function

Onsager, in Eq. (5.10) of his second paper on the reciprocal relations,⁵ gives what he believes is the actual thermodynamic potential whose exponential divided by Boltzmann's constant gives the probability of a transition. It ought to be directly comparable to the second entropy, and in the present notation it is

$$\tilde{\mathcal{O}}(\mathbf{J}, \mathbf{x}) = S^{(1)}(\mathbf{x}) + S^{(1)}(\mathbf{x}') - \frac{\tau}{2} \mathbf{J} \cdot \underline{\underline{A}}^{-1} \mathbf{J}$$

$$= \text{const.} + \tau \mathbf{J} \cdot \mathbf{X} - \frac{\tau}{2} \mathbf{J} \cdot \underline{\underline{A}}^{-1} \mathbf{J}. \quad (2.25)$$

Here an expansion to linear order in the time interval has been performed. It can be seen that this differs by a factor of 2 from the second entropy. In addition it does not correctly take into account the irreversibility of thermodynamic transitions (i.e. the absolute value of the time interval should appear in the final term). These discrepancies arise from the lack of physical justification for Onsager's postulate that the rate of entropy dissipation is maximised. Despite these problems, one can nevertheless observe that this variational function is rather close in spirit to the second entropy approach.

3. Comparison with Onsager's Third Function

Onsager and Machlup,¹⁴ some 20 years after the papers just mentioned, gave a further variational principle that is based upon an expression almost identical to the second entropy expression. In Eq. (4.2), they derive the conditional probability for the scalar transition $x_1 \xrightarrow{\tau} x_2$ from the Langevin equation. The key assumptions, in the present notation, are that the first entropy has fluctuation form (i.e. $S^{(1)}(x) = Sx^2/2$ and $X = Sx$), that the system is Markovian so that the most likely regression is exponential, $\bar{x}_2 = e^{|\tau|VAS}x_1$, and that the stochastic process is stationary and Gaussian. The latter assumption means that the variance of the random Langevin force is fully determined by the entropy and transport constants. This supplies the additional condition needed to fully determine the two non-trivial coefficients for the quadratic variational principle and removes the ambiguity of Onsager's prior versions of the Principle.

It is worth mentioning that a full analysis of stationary, Gaussian, Markov processes, which are also called Ornstein-Uhlenbeck processes, is given by Keizer in §1.8 of Ref. 15. Keizer treats the multi-component Langevin equation, taking into account the non-commutativity of the matrices, and gives the generalised fluctuation-dissipation theorem. The generalised Langevin equation is treated by the present author in Ch. 10 of Ref. 12.

The second entropy corresponding to the exponent of the unconditional probability based on Eq. (4.2)¹⁴ is, in the present notation,

$$\begin{aligned} S_{\text{OM}}^{(2)}(x_2, x_1|\tau) &= S^{(1)}(x_1) + \frac{1}{2} S [1 - e^{2\tau VAS}]^{-1} [x_2 - e^{\tau VAS} x_1]^2 \\ &= S^{(1)}(x_1) - \frac{1}{4V\tau} A^{-1} [1 + \mathcal{O}(\tau)] \\ &\quad \times [x_2 - x_1 - \tau VAS x_1 + \mathcal{O}(\tau^2)]^2 \\ &= S^{(1)}(x_1) - \frac{\tau V}{4} A^{-1} [J - AX_1]^2 + \mathcal{O}(\tau^2). \end{aligned} \quad (2.26)$$

For $\tau > 0$, this may be seen to equal the expression for the second entropy given above, Eq. (2.21). (For $\tau < 0$

this does not correctly account for the irreversibility of the trajectory. Also, whereas Onsager assumed Markov behavior, Eq. (2.21) has been shown to hold as well for non-Markov systems. See §2.3 and §2.4.6 of Ref. 12.)

Onsager and Machlup, in Eq. (4.19) of Ref. 14, recast $S_{\text{OM}}^{(2)}$ as a variational principle for the time integral of the so-called thermodynamic Lagrangian, which involves the dissipation functions ϕ , ψ , and \dot{S} ,

$$\mathcal{O}_3(x_2|x_1, \tau) = \frac{-1}{2} \left\{ \int_{t_1}^{t_2} dt [\phi(\dot{x}(t)) + \psi(X(x(t))) - \dot{S}(\dot{x}(t), X(x(t)))] \right\}_{\min}. \quad (2.27)$$

Minimisation of the integral with respect to the path constrained to fixed values at specified nodes (in this case x_1 and x_2 at t_1 and $t_2 = t_1 + \tau$) yields $S_{\text{OM}}^{(2)}(x_2, x_1|\tau)$. (It is possible to specify values at more than two nodes.) This variational functional is rather common in the field of stochastic differential equations and there are a number of thermodynamic Lagrangians that are based upon it.^{15–22} In particular, the integrand is the negative of the variational principle used by Gyarmati,^{23,24} and it is equal to the thermodynamic Lagrangian given by Lavenda, Eq. (1.17).²⁰ The same criticism may be made of it as of the other variational functions: it has no physical meaning in the constrained state, and it is but one of an infinite family of variational functionals that could be constructed to yield the steady state, but which are physically meaningless more generally.

In any case, it is not entirely clear why one would want to carry out this variational procedure since one already has an explicit expression for both the optimum path between the nodal values and the path entropy for the nodal values. Perhaps Onsager never fully appreciated the second entropy, and instead continued to search for an alternative thermodynamic variational principle for non-equilibrium systems based upon the rate of entropy dissipation. From the point of view of the present author, the thermodynamic principle for non-equilibrium systems is given by the second entropy for transitions, and this is not directly connected to the rate of entropy dissipation.

4. The Point of the Second Entropy

What is the use of the second entropy? Does it give anything beyond the already known reciprocal relations and linear transport laws? One can identify two additional results of significance. First, and conceptually, it provides a rigorous variational principle for non-equilibrium thermodynamics, and one that is unique on physical grounds. This is the analogue of the Second Law of Equilibrium Thermodynamics. Second, and practically, it provides the correct formula for the probability of fluctuations in the fluxes. These are not given by the linear transport laws, and it is this property that makes it the correct non-equilibrium thermodynamic potential.

Beyond these specific consequences, there is more nebulous but possibly more far-reaching outcome of the second entropy approach: it focusses thinking about non-equilibrium systems on the transitions between states rather than on the states themselves. The states may be regarded as the objects of equilibrium thermodynamics and, in contrast, it is the transitions that are the stuff of non-equilibrium thermodynamics. It is this change in mind set that is crucial to providing the insight as to why the Principle of Least Dissipation (or Principle of Maximum Dissipation) cannot provide the basis for non-equilibrium thermodynamics. And, as will be shown explicitly in this paper, it provides a conceptual basis for interpreting not only the specific computational results obtained here for heat convection, but also for understanding in general non-equilibrium phase transitions and pattern formation in non-equilibrium systems.

III. HYDRODYNAMIC EQUATIONS OF CONVECTION

A. Boussinesq Approximation

The Boussinesq approximation is generally invoked for hydrodynamic calculations of convective heat flow.^{25,26} In this the compressibility is set to zero, $\chi_T = 0$, and the thermal expansivity is neglected everywhere except in the buoyancy force. With these the density equation reduces to the vanishing of the divergence of the velocity field,

$$\nabla \cdot \mathbf{v}(\mathbf{r}, t) = 0. \quad (3.28)$$

This means that the most likely value of the scalar part of the viscous pressure tensor vanishes, $\bar{\pi} = 0$.

The gravitational potential density is

$$n(\mathbf{r}, t)\psi(\mathbf{r}, t) = \{n_{00} - \alpha n_{00}[T_{\text{tot}}(\mathbf{r}, t) - T_{00}]\} mgz. \quad (3.29)$$

Here α is the thermal expansivity, g is the acceleration due to gravity, and m is the molecular mass. The subscript tot signifies the total temperature, $T_{\text{tot}} = T_0 + T$, where T_0 is the temperature in conduction, and T is convective perturbation. The subscript 00 denotes the reference value at the mid-point of the sub-system, and everything will be expanded to linear order in the difference from this reference point. Inserting this in the Navier-Stokes equation and neglecting the term quadratic in the velocity yields

$$mn_{00} \frac{\partial \mathbf{v}(\mathbf{r}, t)}{\partial t} = - \{n_{00} - \alpha n_{00}[T_{\text{tot}}(\mathbf{r}, t) - T_{00}]\} mg\hat{\mathbf{z}} - \nabla p_{\text{tot}}(\mathbf{r}, t) + \eta \nabla^2 \mathbf{v}(\mathbf{r}, t), \quad (3.30)$$

where η is the shear viscosity.

Neglecting the viscous dissipation, which is quadratic in the velocity, and also the thermal expansivity, and

using the most likely heat flux, the energy equation becomes

$$c_p \frac{\partial T_{\text{tot}}(\mathbf{r}, t)}{\partial t} + c_p \mathbf{v}(\mathbf{r}, t) \cdot \nabla T_{\text{tot}}(\mathbf{r}, t) = \lambda \nabla^2 T_{\text{tot}}(\mathbf{r}, t), \quad (3.31)$$

where λ is the thermal conductivity. The coupling of velocity and temperature represents a non-linear term. These three partial differential equations constitute the Boussinesq approximation that is to be solved for the temperature, pressure, and velocity fields.

B. Conduction

The simplest case of slab geometry is treated here, with a temperature gradient imposed in the z -direction. The convective flow is treated as a perturbation from the conducting state. In conduction, the velocity field is zero, $\mathbf{v}(\mathbf{r}, t) = 0$.

The boundaries of the sub-system are located at $z = \pm L_z/2$, and the temperatures of the reservoirs beyond the boundaries are $T_{r\pm}$. The temperature difference is $\Delta_T \equiv T_{r+} - T_{r-}$. It is assumed that the imposed temperature gradient, Δ_T/L_z , is small and that quadratic terms can be neglected. This means that it does not matter whether one deals with the difference in temperature or with the difference in inverse temperature. For convection to occur, the lower reservoir must be hotter than the upper reservoir, $\Delta_T < 0$.

Since in conduction the velocity vanishes, and the temperature is steady and a function of z only, the energy equation reduces to

$$0 = \lambda \frac{d^2 T_0(z)}{dz^2}. \quad (3.32)$$

Hence the temperature field is a linear function of z that must equal the reservoirs' temperatures at the boundaries,

$$T_0(z) = T_{00} + \frac{\Delta_T}{L_z} z, \quad |z| \leq L_z/2, \quad (3.33)$$

with the mid-point temperature being $T_{00} \equiv [T_{r+} + T_{r-}]/2$. With this and zero velocity, the Navier-Stokes equation becomes

$$0 = - \left\{ n_{00} - \frac{\alpha n_{00} \Delta_T}{L_z} z \right\} mg - \frac{dp_0(z)}{dz}. \quad (3.34)$$

Hence the pressure profile in conduction is

$$p_0(z) = p_{00} - n_{00} mg z + \frac{\alpha n_{00} mg \Delta_T}{2L_z} z^2. \quad (3.35)$$

For future use, the heat flow per unit area in conduction is

$$\overline{J_{E,0}^0} = -\lambda \frac{dT_0(z)}{dz} = \frac{-\lambda \Delta_T}{L_z}. \quad (3.36)$$

The rate of entropy production per unit sub-system volume is

$$\dot{S}_r/AL_z = \frac{\overline{J_{E,0}^0}}{L_z} \left[\frac{1}{T_{r+}} - \frac{1}{T_{r-}} \right] = \frac{\lambda \Delta_T^2}{T_{00}^2 L_z^2}. \quad (3.37)$$

This is positive and independent of the sign of the temperature difference, as it ought to be.

C. Convection

Regarding convection as a perturbation on conduction, the temperature may be written

$$T_{\text{tot}}(\mathbf{r}, t) = T_0(z) + T(\mathbf{r}, t), \quad (3.38)$$

and similarly the pressure,

$$p_{\text{tot}}(\mathbf{r}, t) = p_0(z) + p(\mathbf{r}, t). \quad (3.39)$$

Since the velocity is zero in conduction, the full velocity field is the same as the perturbing velocity field, $\mathbf{v}_{\text{tot}}(\mathbf{r}, t) = \mathbf{v}(\mathbf{r}, t)$. These convective fields depend upon the Rayleigh number and, in the calculations below, the wave number of the steady state being characterised, but these will not be shown explicitly.

The full fields satisfy the density, Navier-Stokes, and energy equations. But since the conductive fields also satisfy these equations, they can be subtracted from both sides, so that one has

$$0 = \nabla \cdot \mathbf{v}(\mathbf{r}), \quad (3.40)$$

$$mn_{00} \frac{\partial \mathbf{v}(\mathbf{r}, t)}{\partial t} = \alpha n_{00} T(\mathbf{r}) mg \hat{\mathbf{z}} - \nabla p(\mathbf{r}) + \eta \nabla^2 \mathbf{v}(\mathbf{r}), \quad (3.41)$$

and

$$\begin{aligned} c_p \frac{\partial T(\mathbf{r}, t)}{\partial t} &= -c_p \mathbf{v}(\mathbf{r}) \cdot \nabla [T_0(z) + T(\mathbf{r})] + \lambda \nabla^2 T(\mathbf{r}) \\ &= -\frac{c_p \Delta_T}{L_z} v_z(\mathbf{r}) - c_p \mathbf{v}(\mathbf{r}) \cdot \nabla T(\mathbf{r}) + \lambda \nabla^2 T(\mathbf{r}). \end{aligned} \quad (3.42)$$

In the steady state the left-hand sides are zero. Here the left hand side of the final term will be retained as non-zero. This is useful both as an iterative device (simple time stepping) for the computer algorithm to obtain a converged steady state solution, and also to obtain the physical properties of the system during the evolution in time either from conduction to convection or during the transition from one convecting state to another. This implicitly assumes rapid relaxation of the velocity at each time step, $\partial \mathbf{v} / \partial t = 0$.

If one regards the convective perturbation as small, then one sees that the second term on the right-hand side of the energy equation is non-linear, as it is the product

of the convective temperature and the velocity. This non-linear term fixes the amplitude of the fields that give the steady state, since without it everything could be multiplied by a constant to give another solution. There are five equations (the Navier-Stokes equation is for three components) and five fields, including the three components of the velocity.

Now use L_z as the unit of length, $-\Delta_T$ as the unit of temperature, $L_z^2 c_p / \lambda$ as the unit of time, and $mn_{00} \lambda^2 / L_z^2 c_p^2$ as the unit of pressure. Denoting dimensionless quantities with an asterisk, one has

$$0 = \nabla^* \cdot \mathbf{v}^*, \quad (3.43)$$

$$\frac{\partial \mathbf{v}^*}{\partial t^*} = \mathcal{R} P T^* \hat{\mathbf{z}} - \nabla^* p^* + \mathcal{P} \nabla^{*2} \mathbf{v}^*, \quad (3.44)$$

and

$$\frac{\partial T^*}{\partial t^*} = v_z^* - \mathbf{v}^* \cdot \nabla^* T^* + \nabla^{*2} T^*. \quad (3.45)$$

Here the Rayleigh number is

$$\mathcal{R} \equiv -\Delta_T \alpha g c_p m n_{00} L_z^3 / \lambda \eta, \quad (3.46)$$

and the Prandtl number is

$$\mathcal{P} \equiv \eta c_p / m n_{00} \lambda. \quad (3.47)$$

Here and throughout, c_p is the constant pressure heat capacity per unit volume.

One can eliminate the pressure from the Navier-Stokes equations. Set the left-hand side to zero, differentiate the z -component with respect to y , the y -component with respect to z , and subtract,

$$0 = \mathcal{R} \frac{\partial \tilde{T}^*}{\partial y^*} + \nabla^{*2} \left[\frac{\partial v_z^*}{\partial y^*} - \frac{\partial v_y^*}{\partial z^*} \right]. \quad (3.48)$$

The Prandtl number has been factored out. Similarly for the x -component,

$$0 = \mathcal{R} \frac{\partial \tilde{T}^*}{\partial x^*} + \nabla^{*2} \left[\frac{\partial v_z^*}{\partial x^*} - \frac{\partial v_x^*}{\partial z^*} \right]. \quad (3.49)$$

One now has four equations (these two forms of the momentum equation, the density equation, and the energy equation), four fields (T^* , v_x^* , v_y^* , and v_z^*), and one dimensionless parameter, \mathcal{R} . Since everything in these equations is dimensionless and refers to the convective perturbation, the asterisk will be dropped later below.

IV. TOTAL FIRST ENTROPY OF CONVECTION

Now an expression for the first or structural entropy of a convecting steady state will be obtained as the difference from the conducting state. (Quite generally the

free energy is minus the temperature times the total first entropy,²⁷ and so the following results could be recast in terms of free energy, if desired.) The total entropy is the sum of the sub-system entropy and the reservoir entropy. Here the exact sub-system entropy will be given, and two forms for the reservoir contribution will be obtained. One reservoir expression is the exact change in reservoir entropy during the transition from one state to another (e.g. conduction to convection, or from one convecting state to another). The second reservoir expression is the so-called static approximation. It gives the difference in reservoir entropy between a convecting state and the conducting state, and again it can be used to obtain the difference in reservoir entropy between one convecting state and another.

The static approximation for the reservoir entropy in a non-equilibrium system was originally presented in Ref. 28, and its nature is discussed in full detail in Ch. 9 of Ref. 12. Briefly, the first entropy for phase space for a non-equilibrium system consists of a static part, which is the analogue of the usual equilibrium expression, and a dynamic part, which is a correction to the static reservoir contribution that accounts for the adiabatic evolution that is unavoidably included. In the present macroscopic description, the sub-system entropy is given exactly by the usual equilibrium expression, which will be obtained explicitly. The non-equilibrium reservoir entropy will be approximated by neglecting the dynamic part and using the static part alone.

The change (or difference) in entropy density of the sub-system between convection and conduction can be obtained by thermodynamic integration of the temperature from that in conduction, $T_0(z) = T_{00} + z \Delta_T / L_z$, to that in convection $T_{\text{tot}}(\mathbf{r}) = T_0(z) + T(\mathbf{r})$. (The dependence of the temperature field (and of the change in entropy) on the Rayleigh number and on the wave number of the particular convective state is not shown explicitly. Also, dimensionless variables are *not* used in this section.) Henceforth this will simply be called the convective entropy density, the change from conduction being understood. Assuming, as in the Boussinesq approximation, that the thermal expansivity and compressibility can be neglected, the convective entropy density of the sub-system is

$$\begin{aligned} \sigma_s(\mathbf{r}) &= \int_{\varepsilon_{\text{int},0}}^{\varepsilon_{\text{int},1}} d\varepsilon'_{\text{int}} \frac{\partial \sigma(\varepsilon'_{\text{int}})}{\partial \varepsilon'_{\text{int}}} \\ &= \int_{\varepsilon_{\text{int},0}}^{\varepsilon_{\text{int},1}} d\varepsilon'_{\text{int}} \frac{1}{T'} \\ &= c_p \ln \left[\frac{T_0(z) + T(\mathbf{r})}{T_0(z)} \right] \\ &= c_p \left[\frac{T(\mathbf{r})}{T_0(z)} - \frac{T(\mathbf{r})^2}{2T_0(z)^2} + \dots \right] \\ &= c_p \left[\frac{T(\mathbf{r})}{T_{00}} - \frac{z \Delta_T T(\mathbf{r})}{L_z T_{00}^2} - \frac{T(\mathbf{r})^2}{2T_{00}^2} + \mathcal{O}(\Delta_T^3 / T_{00}^3) \right]. \end{aligned} \quad (4.50)$$

This uses the fact that $\Delta\varepsilon_{\text{int}} = c_p \Delta T$, where c_p is the heat capacity per unit volume. Since the convective temperature is $T(\mathbf{r}) \sim \mathcal{O}(\Delta T)$, the expansion to quadratic order in the temperature difference is justified. (This expansion has been checked numerically against the full logarithm and found to be accurate for ideal straight rolls over the full range of Rayleigh numbers and wave numbers.) This is the local sub-system entropy density. The global sub-system entropy density is

$$\sigma_s(t) = \frac{1}{AL_z} \int d\mathbf{r} \sigma_s(\mathbf{r}, t), \quad (4.51)$$

where A is the cross-sectional area of the sub-system. For use below during convective transitions, this has been written as a function of time and invokes the instantaneous temperature, $T(\mathbf{r}, t)$.

1. Static Reservoir Entropy

The zeroth and first temperatures of the reservoirs are²⁹

$$\frac{1}{T_{r0}} = \frac{1}{2} \left[\frac{1}{T_{r+}} + \frac{1}{T_{r-}} \right] = \frac{1}{T_{00}} + \mathcal{O}(\Delta_T^2/T_{00}^2), \quad (4.52)$$

and

$$\frac{1}{T_{r1}} = \frac{1}{L_z} \left[\frac{1}{T_{r+}} - \frac{1}{T_{r-}} \right] = \frac{-\Delta T}{L_z T_{00}^2} + \mathcal{O}(\Delta_T^3/T_{00}^3), \quad (4.53)$$

respectively. These correspond in essence to the average temperature and to the temperature gradient of the reservoirs. With these, the static part of the reservoir entropy associated with the sub-system is

$$S_{r,\text{st}} = \frac{-\Delta E_0}{T_{r0}} - \frac{\Delta E_1}{T_{r1}}. \quad (4.54)$$

Again it is understood that this is the change from conduction. The energy moments of the sub-system are defined as

$$\Delta E_n = \int d\mathbf{r} z^n \Delta\varepsilon(\mathbf{r}). \quad (4.55)$$

In view of this one can define the static convective reservoir entropy density,

$$\sigma_{r,\text{st}}(\mathbf{r}) \equiv \frac{-\Delta\varepsilon(\mathbf{r})}{T_{r0}} - \frac{z\Delta\varepsilon(\mathbf{r})}{T_{r1}}. \quad (4.56)$$

What appears here is the change in total energy density, which is composed of the internal energy density, the gravitational energy density, and the kinetic energy density,

$$\begin{aligned} \Delta\varepsilon(\mathbf{r}) &= \Delta\varepsilon_{\text{int}}(\mathbf{r}) + \Delta\varepsilon_g(\mathbf{r}) + \Delta\varepsilon_{\text{ke}}(\mathbf{r}) \\ &= c_p T(\mathbf{r}) - \alpha m n_{00} g z T(\mathbf{r}) + \frac{m n_{00}}{2} \mathbf{v}(\mathbf{r}) \cdot \mathbf{v}(\mathbf{r}). \end{aligned} \quad (4.57)$$

Accordingly, the change in total entropy density, $\sigma_{\text{tot,st}}(\mathbf{r}) = \sigma_s(\mathbf{r}) + \sigma_{r,\text{st}}(\mathbf{r})$, is composed of three analogous terms. The internal energy density contribution includes the sub-system entropy and is

$$\begin{aligned} \sigma_{\text{tot,st}}^{\text{int}}(\mathbf{r}) &\equiv \sigma_s(\mathbf{r}) - \frac{\Delta\varepsilon_{\text{int}}(\mathbf{r})}{T_{r0}} - \frac{z\Delta\varepsilon_{\text{int}}(\mathbf{r})}{T_{r1}} \\ &= c_p \left[\frac{T(\mathbf{r})}{T_{00}} - \frac{z\Delta_T T(\mathbf{r})}{L_z T_{00}^2} - \frac{T(\mathbf{r})^2}{2T_{00}^2} \right] \\ &\quad - \frac{c_p T(\mathbf{r})}{T_{00}} + \frac{c_p z \Delta_T T(\mathbf{r})}{L_z T_{00}^2} \\ &= \frac{-c_p}{2T_{00}^2} T(\mathbf{r})^2. \end{aligned} \quad (4.58)$$

This is identical to the equilibrium fluctuation expression for the total entropy density of a sub-system in equilibrium with a reservoir of temperature T_{00} when the local fluctuation in energy is $\Delta\varepsilon_{\text{int}}(\mathbf{r}) = c_p T(\mathbf{r})$. It is what one would have expected and could have been written down directly. The fact that this is always negative means that a convecting steady state has lower total entropy than the conducting state, at least as far as the rearrangement of the internal energy in the convecting system is concerned. This latter observation is not particularly significant because the result depends upon the static approximation, and so it does not give the full change in the reservoir entropy during such a transition.

The gravitational contribution is

$$\begin{aligned} \sigma_{\text{tot,st}}^g(\mathbf{r}) &\equiv -\frac{\Delta\varepsilon_g(\mathbf{r})}{T_{r0}} - \frac{z\Delta\varepsilon_g(\mathbf{r})}{T_{r1}} \\ &= \frac{\alpha m n_{00} g z T(\mathbf{r})}{T_{00}} - \frac{\alpha m n_{00} g z^2 \Delta_T T(\mathbf{r})}{L_z T_{00}^2}, \end{aligned} \quad (4.59)$$

and the kinetic energy contribution is

$$\begin{aligned} \sigma_{\text{tot,st}}^{\text{ke}}(\mathbf{r}) &\equiv -\frac{\Delta\varepsilon_{\text{ke}}(\mathbf{r})}{T_{r0}} - \frac{z\Delta\varepsilon_{\text{ke}}(\mathbf{r})}{T_{r1}} \\ &= -\frac{m n_{00}}{2T_{00}} \mathbf{v}(\mathbf{r}) \cdot \mathbf{v}(\mathbf{r}) + \frac{m n_{00} \Delta_T z}{2L_z T_{00}^2} \mathbf{v}(\mathbf{r}) \cdot \mathbf{v}(\mathbf{r}). \end{aligned} \quad (4.60)$$

In the case of ideal straight rolls, there is an up-down symmetry so that the convective temperature perturbation is anti-symmetric upon reflection through the center of a convective roll. This means that the final term on the right-hand side of each of these integrates to zero.

The sum of the last three results represent the static approximation to the convective entropy density (i.e. the difference in entropy between the convective state and the conductive state). Integrating over the volume of the sub-system, the global convective entropy density is

$$\sigma_{\text{tot,st}} \equiv \frac{1}{AL_z} \int d\mathbf{r} [\sigma_{\text{tot,st}}^{\text{int}}(\mathbf{r}) + \sigma_{\text{tot,st}}^g(\mathbf{r}) + \sigma_{\text{tot,st}}^{\text{ke}}(\mathbf{r})]. \quad (4.61)$$

2. Change in Reservoir Entropy

The reservoir contribution to the above result for the convection entropy is approximate, whereas the sub-system entropy is exact. However, by integrating over time the heat flow through the sub-system from one reservoir to the other, one can obtain exactly the change in reservoir entropy for a transition between two non-equilibrium states.

The formally exact rate of change of the entropy of the reservoirs is

$$\begin{aligned}\dot{S}_r(t) &= \int_A dx dy \left[\frac{1}{T_{r+}} \bar{J}_E^0(x, y, L_z/2, t) \right. \\ &\quad \left. - \frac{1}{T_{r-}} \bar{J}_E^0(x, y, -L_z/2, t) \right] \\ &\approx \frac{-L_z \Delta T}{T_{00}^2} \int_A dx dy \bar{J}_E^0(x, y, L_z/2, t) \\ &= \frac{-L_z \Delta T \lambda}{T_{00}^2} \int_A dx dy \left. \frac{\partial T(\mathbf{r}, t)}{\partial z} \right|_{z=L_z/2} \quad (4.62)\end{aligned}$$

The first equality is exact, whereas the second equality makes the approximation that the integrated heat flux at the two boundaries are equal. This is certainly the case in the steady state, and it is a very good approximation in the transitions between steady straight roll states that are characterised below. This approximation does not account for any nett total energy change of the sub-system during a transition, such as those in the gravitational energy and in the kinetic energy, but these are negligible compared to the total heat flux over the time interval of a transition. Using this, the change in total entropy per unit sub-system volume during a transition over the time interval $[t_1, t_2]$ is

$$\Delta \sigma_{\text{tot}} = \sigma_s(t_2) - \sigma_s(t_1) + \frac{1}{AL_z} \int_{t_1}^{t_2} dt \dot{S}_r(t), \quad (4.63)$$

where the global sub-system entropy density is given by Eq. (4.51).

V. IDEAL STRAIGHT ROLLS

This and the following section set out the hydrodynamic equations used for convection and describes the computer algorithms that were used to solve them. This section deals with ideal straight rolls (i.e. the rolls are considered straight and homogeneous in the x -direction), and the next section deals with the cross roll state (i.e. the combination of straight x - and y -rolls).

The applied thermal gradient and gravity are in the z -direction. The wavelength is twice the width of an individual roll, $\Lambda = 2L_y$, as they come in pairs of counter-rotating rolls, and the wave number is defined as $a = 2\pi/\Lambda$.

In this and the following sections, dimensionless variables are used, with the asterisk being dropped. Hence

$L_y = 1$ or $a \approx 3.1$ corresponds to a roll whose width and height are approximately equal.

A. Hydrodynamic Equations

The hydrodynamic equations for convection were given at the end of §III C. For the present ideal straight rolls with their axis in the x -direction, the x -component of velocity and the x -derivatives are zero. The three equations for the remaining three fields are

$$0 = \frac{\partial v_y(y, z)}{\partial y} + \frac{\partial v_z(y, z)}{\partial z}, \quad (5.64)$$

$$\begin{aligned}\frac{\partial T(y, z)}{\partial t} &= v_z(y, z) - v_y(y, z) \frac{\partial T(y, z)}{\partial y} - v_z(y, z) \frac{\partial T(y, z)}{\partial z} \\ &\quad + \frac{\partial^2 T(y, z)}{\partial y^2} + \frac{\partial^2 T(y, z)}{\partial z^2}, \quad (5.65)\end{aligned}$$

and

$$\begin{aligned}0 &= \mathcal{R} \frac{\partial T(y, z)}{\partial y} + \nabla^2 \left[\frac{\partial v_z(y, z)}{\partial y} - \frac{\partial v_y(y, z)}{\partial z} \right] \\ &= \mathcal{R} \frac{\partial^2 T(y, z)}{\partial y^2} + \left[\frac{\partial^2}{\partial y^2} + \frac{\partial^2}{\partial z^2} \right]^2 v_z(y, z). \quad (5.66)\end{aligned}$$

The second equality follows by taking the y -derivative of the first equality and using the vanishing of the divergence of the velocity. Recall that the Rayleigh number is $\mathcal{R} \equiv -\alpha m g n_{00} c_p \Delta T L_z^3 / \lambda \eta$.

B. Fourier Expansion

Following Busse,³⁰ a Galerkin method is used that invokes Fourier expansions of the fields. The temperature field is expanded as

$$\begin{aligned}T(y, z) &= \sum_{l=0}^L \sum_{n=1}^N [T_{ln}^s \sin 2n\pi z \\ &\quad + T_{ln}^c \cos(2n-1)\pi z] \cos lay. \quad (5.67)\end{aligned}$$

The form of the z -expansion is chosen to guarantee the boundary conditions, $T(y, \pm 1/2) = 0$. For the Boussinesq fluid, there is mirror plane symmetry between two rolls, $T(y, z) = T(-y, z)$, and point reflection symmetry within a roll, $T(y, z) = -T(L_y - y, -z)$. These mean that the even l coefficients of T_{ln}^s and the odd l coefficients of T_{ln}^c must vanish.

The particular solution of the differential equation for the velocity is

$$\begin{aligned}v_z^p(y, z) &= \sum_{l,n} \left[v_{z,ln}^{\text{ps}} \sin 2n\pi z \right. \\ &\quad \left. + v_{z,ln}^{\text{pc}} \cos(2n-1)\pi z \right] \cos lay. \quad (5.68)\end{aligned}$$

Clearly,

$$v_{z,ln}^{\text{ps}} = \frac{\mathcal{R}(la)^2}{[(la)^2 + (2n\pi)^2]^2} T_{ln}^{\text{s}}, \quad (5.69)$$

and

$$v_{z,ln}^{\text{pc}} = \frac{\mathcal{R}(la)^2}{[(la)^2 + ((2n-1)\pi)^2]^2} T_{ln}^{\text{c}}. \quad (5.70)$$

The homogeneous solution, which satisfies $\nabla^2 \nabla^2 v_z^{\text{h}} = 0$, is

$$v_z^{\text{h}}(y, z) = \sum_{l=1}^L [A_l^{\text{s}} \sinh laz + B_l^{\text{s}} z \cosh laz + A_l^{\text{c}} \cosh laz + B_l^{\text{c}} z \sinh laz] \cos lay. \quad (5.71)$$

Because the system is periodic in the horizontal direction, there is a term for each expansion mode. Writing the velocity as $v_z = v_z^{\text{p}} + v_z^{\text{h}}$, the four boundary conditions for each mode, $v_z(y, \pm 1/2) = \partial v_z(y, \pm 1/2)/\partial z = 0$, determine the four coefficients per mode, A_l^{s} , B_l^{s} , A_l^{c} , and B_l^{c} . These coefficients have the Boussinesq symmetry discussed above. The second condition ensures the vanishing of $v_y(y, \pm 1/2)$ when the density equation is applied.

The vertical velocity field is then projected onto the Fourier grid used for the temperature field using the orthogonality of the trigonometric functions. Formally one has

$$v_z(y, z) = \sum_{l=1}^L \sum_{n=1}^N [v_{z,ln}^{\text{s}} \sin 2n\pi z + v_{z,ln}^{\text{c}} \cos(2n-1)\pi z] \cos lay. \quad (5.72)$$

Due to the Boussinesq symmetry, half the coefficients are zero. The horizontal velocity may be expanded as

$$v_y(y, z) = \sum_{l=1}^L \sum_{n=1}^N [v_{y,ln}^{\text{c}} \cos 2n\pi z + v_{y,ln}^{\text{s}} \sin(2n-1)\pi z] \sin lay. \quad (5.73)$$

The density equation gives

$$v_{y,ln}^{\text{c}} = \frac{-2n\pi}{la} v_{z,ln}^{\text{s}} \text{ and } v_{y,ln}^{\text{s}} = \frac{(2n-1)\pi}{la} v_{z,ln}^{\text{c}}. \quad (5.74)$$

The rates of change of the temperature coefficients are obtained from the non-linear energy equation, Eq. (5.65), again using trigonometric orthogonality. The left-hand side of this equation is $\partial T/\partial t$, which is non-zero in the approach to the steady state. Hence one can update the temperature field by simple time stepping, with the new temperature coefficients obtained by adding a constant $\Delta_t \sim \mathcal{O}(10^{-4})$ times the right-hand side to the previous value.

Linear stability analysis reveals that the critical Rayleigh number is $\mathcal{R}_c = 1708$ and the critical wave number is $a_c = 3.117$.^{25,26} For a given Rayleigh number $\mathcal{R} > \mathcal{R}_c$, there is a range of wave numbers a that yield steady state solutions. These are the neutrally stable states. Of these, some wave numbers are unstable to the cross roll and other transitions.

C. Nusselt Number

The Nusselt number is the ratio of the total heat flux in convection to that in conduction at a given Rayleigh number. The heat flux in conduction is just Fourier's law, $J_{\text{E}}^{\text{cond}} = -\lambda \Delta_T$. Since the velocity vanishes at the horizontal boundaries, the heat flux in convection is purely conductive across these boundaries. Integrating over a single convection cell, the Nusselt number is

$$\begin{aligned} \mathcal{N} &= \frac{1}{L_y J_{\text{E}}^{\text{cond}}} \int_{-L_y}^0 dy (-\lambda) \left. \frac{\partial T^{\text{total}}(y, z)}{\partial z} \right|_{z=\pm 1/2} \\ &= 1 - \sum_{n=1}^N T_{0n}^{\text{s}} 2n\pi (-1)^n. \end{aligned} \quad (5.75)$$

The temperature in the integrand is the sum of the conductive temperature field plus the convective perturbation, Eq. (3.38). The conductive part gives rise to the first term, 1, and the convective terms involving $\sin 2n\pi z$ and $l = 0$ give rise to the remainder.

D. Algorithms

1. Stable States

The Fourier expansion of the temperature and velocity fields in conjunction with the hydrodynamic equations given above were used to develop two different algorithms for ideal straight roll convection. The first algorithm was used to characterise neutrally stable straight roll convection. For each such steady state, single time quantities such as the temperature and velocity fields, the heat flow, Eq. (5.75), and the static part of the total entropy, Eq. (4.61), were determined. In this first ideal straight roll case, a wave number a typically in the neutrally stable range $[2, 10]$ was chosen, with $L \approx N \approx 10$. Neutrally stable means that a steady state ideal straight roll solution exists at that wave number and Rayleigh number. This solution might be unstable to perturbations, either to straight roll states with a different wave numbers, or to other convecting patterns.

The algorithm proceeded using the equations give above with simple time stepping, $T_{ln}^{\text{s/c}}(t + \Delta_t) = T_{ln}^{\text{s/c}}(t) + \Delta_t \dot{T}_{ln}^{\text{s/c}}(t)$. Usually, the initial point was chosen as a small non-zero value in some low order modes, for example $T_{0,1}^{\text{s}} = T_{1,1}^{\text{c}} = 10^{-3}$. No changes to the results were observed using other starting points. In some cases, particularly at higher Rayleigh numbers or toward the extremities of the neutrally stable range, a previously converged steady state solution at a nearby wave number or Rayleigh number was used as the starting point. When converged, the final steady state represented ideal straight roll convection parallel to the y -axis of wavelength $\Lambda = 2\pi/a$. Most of the power was in the fundamental mode a , with the next most prominent mode

TABLE I: Measured (silicone oil, $\mathcal{P} = 930$) and computed velocity amplitudes, ($\mu\text{m/s}$), for the first three harmonics[†] at $a = 3.117$ and two Rayleigh numbers.

	Measured ³¹ $\mathcal{R} = 3416$	Busse ³¹	Present	Measured ³¹ $\mathcal{R} = 11,391$	Present
V_y^1	132 ± 4	133	137.6	337 ± 10	355.1
V_y^2	$5.3 \pm 0.5^\ddagger$	5^\ddagger	5.1^\ddagger	13.7 ± 1	13.0
V_y^3	1.5 ± 0.3	-	1.2	19 ± 1	18.3
V_z^1	145 ± 5	138	140.6	340 ± 10	363.0
V_z^2	0	0	0	1.7 ± 2	0
V_z^3	4 ± 0.4	3.8	3.9	58 ± 4	60.2

[†]The V_z are at $z^{**} = 0$, and the V_y are at $z^* = 0.28$.

[‡]At $z^* = 0$.

being $3a$. In this type of calculation the fixed wave number determines the final steady state. It is most useful for obtaining thermodynamic properties as a function of the steady state wave number, for example, the heat flux, the static part of the entropy, and the velocity fields.

The Nusselt number was monitored and used to halt the iterative procedure when its relative change was less than 10^{-5} . For many of the results reported below, $N = 10$ and $L = 10$. Some tests were carried out with up to $N = 16$ and $L = 16$. By comparison, Busse³⁰ used up to $L + N = 12$. In general, three- or four- figure agreement was obtained between the present results and those of Busse for Rayleigh numbers up to 30,000.

The amplitudes of the first three harmonics of the velocity field in convection have been measured by Dubois and Bergé for a silicone oil ($\mathcal{P} = 930$) constrained at the critical wavelength.^{31,32} Their results are shown in Table I, together with their reports of the results of Busse's calculations, and with the results of the present calculations, which should be equivalent to those of Busse (apart from the non-linear influence of the greater number of modes used here). There is quite good agreement between all three, which confirms both the validity of the present computational algorithm and the applicability of the hydrodynamic model to the experimental situation.

2. Conduction-Convection Transition

In the second type of straight roll calculation, a small wave number was chosen as the fundamental, $a \approx 0.2$ – 0.5 , and a large number of modes were used, $L \approx 60$ – 100 and $N \approx 10$. A number of different initial states were tested including uniform distributions as well as Gaussian distributions of the temperature coefficients, and white noise. It was found that the system converged to a straight roll steady state that was an odd harmonic of the small wave number, $\bar{a} = (2\bar{l} + 1)a$. (The odd harmonic is demanded by the Boussinesq symmetry.) The final mode was identified from the power spectrum.

It was confirmed that the properties of the convecting state given by this second algorithm were equal to those given by the first algorithm with fundamental wave number equal to \bar{a} .

This second type of calculation modeled the conduction to straight roll convection transition. Whereas the first calculation tells the possible straight roll steady states at a given Rayleigh number, the second calculation tells the most likely straight roll steady state that results from a transition directly from the conducting state at a given Rayleigh number. The modal power, the sub-system entropy, and the reservoir entropy were monitored as a function of time during the transition.

At each Rayleigh number 6–19 independent trials were performed. The most likely wave number \bar{a} for each trial was recorded (this is the most likely out of all possible wave numbers la), as well as the average of these over all the trials, $\langle \bar{a} \rangle$.

It is important to note that the outcome of this second algorithm does not refer to the most likely (or average) state, but rather to the most likely (or average) transition from the conducting state. This appears to be a general point that will be confirmed in the results given below: for non-equilibrium systems, one cannot speak of *the* most likely phase, but only of the optimum transition from the current phase.

VI. CROSS ROLL STATE

A. Hydrodynamic Equations and Conditions

This section sets out the computational algorithm that is used for cross roll convection. It is supposed that the system is periodic in the x and y directions, $T(x, y, z) = T(x + m\Lambda_x, y + n\Lambda_y, z)$, $m, n = \pm 1, \pm 2, \dots$. The wavelength is twice the width of an individual roll, as they come in counter-rotating pairs, $\Lambda_x = 2L_x$ and $\Lambda_y = 2L_y$. The wave numbers are given by $\Lambda_x = 2\pi/a_x$, and $\Lambda_y = 2\pi/a_y$.

The four hydrodynamic equations for the four fields, (temperature and three velocity components) are explicitly

$$0 = \frac{\partial v_x}{\partial x} + \frac{\partial v_y}{\partial y} + \frac{\partial v_z}{\partial z}, \quad (6.76)$$

$$\begin{aligned} \frac{\partial T}{\partial t} = & v_z + \frac{\partial^2 T}{\partial x^2} + \frac{\partial^2 T}{\partial y^2} + \frac{\partial^2 T}{\partial z^2} \\ & - v_x \frac{\partial T}{\partial x} - v_y \frac{\partial T}{\partial y} - v_z \frac{\partial T}{\partial z}, \end{aligned} \quad (6.77)$$

$$0 = \mathcal{R} \frac{\partial T}{\partial x} + \nabla^2 \left[\frac{\partial v_z}{\partial x} - \frac{\partial v_x}{\partial z} \right], \quad (6.78)$$

and

$$0 = \mathcal{R} \frac{\partial T}{\partial y} + \nabla^2 \left[\frac{\partial v_z}{\partial y} - \frac{\partial v_y}{\partial z} \right]. \quad (6.79)$$

Taking the x derivative of the penultimate equation, the y derivative of the final equation, using the density equation, and adding them together gives,

$$\begin{aligned} 0 &= \mathcal{R} \left[\frac{\partial^2}{\partial x^2} + \frac{\partial^2}{\partial y^2} \right] T + \left[\frac{\partial^2}{\partial x^2} + \frac{\partial^2}{\partial y^2} + \frac{\partial^2}{\partial z^2} \right]^2 v_z \\ &\equiv \mathcal{R} \nabla_{\parallel}^2 T + \nabla^2 \nabla^2 v_z. \end{aligned} \quad (6.80)$$

In all these equations, the temperature and velocity fields are all functions of the position, $\mathbf{r} = \{x, y, z\}$. In the steady state they are not functions of time, but in a transition between states they are.

1. Boundary Conditions

The temperature that appears here is the perturbation due to convection. That is, the conductive solution has been subtracted from these equations. This means that the temperature perturbation must vanish at the upper and lower boundaries,

$$T(x, y, \pm 1/2) = 0. \quad (6.81)$$

Since no fluid can cross the boundaries one must also have

$$v_z(x, y, \pm 1/2) = 0. \quad (6.82)$$

The boundaries are solid walls at which the fluid sticks, so that one also has

$$v_x(x, y, \pm 1/2) = v_y(x, y, \pm 1/2) = 0. \quad (6.83)$$

Since this last equation implies that $\partial v_x(x, y, \pm 1/2)/\partial x = \partial v_y(x, y, \pm 1/2)/\partial y = 0$, the density equation implies that $\partial v_z(x, y, z)/\partial z|_{z=\pm 1/2} = 0$.

2. Symmetry

The fundamental convection cell, $-L_x \leq x \leq L_x$ and $-L_y \leq y \leq L_y$, contains two counter rotating rolls in each direction. Hence there is mirror plane symmetry at $x = 0$ and at $y = 0$. This means that

$$\begin{aligned} T(x, y, z) &= T(-x, y, z) = T(x, -y, z), \\ v_x(x, y, z) &= -v_x(-x, y, z) = v_x(x, -y, z), \\ v_y(x, y, z) &= v_y(-x, y, z) = -v_y(x, -y, z), \\ v_z(x, y, z) &= v_z(-x, y, z) = v_z(x, -y, z). \end{aligned} \quad (6.84)$$

These mean that the expansion for the temperature must be even in the lateral coordinates, and so must consist of terms like $T_{qp}(z) \cos(qa_x x) \cos(pa_y y)$, q and p being non-negative integers. A similar expansion holds for v_z . Obviously for v_x and v_y the respective cosine is replaced by a sine.

The Boussinesq symmetry refers to the reflection symmetry within a roll. For $\mathbf{r} = \{x, y, z\}$, define $\mathbf{r}^\dagger = \{L_x - x, L_y - y, -z\}$. One must have

$$T(\mathbf{r}) = -T(\mathbf{r}^\dagger), \text{ and } \mathbf{v}(\mathbf{r}) = -\mathbf{v}(\mathbf{r}^\dagger). \quad (6.85)$$

These basically say that the convective temperature perturbation at the top of an up draught must be equal and opposite to that at the bottom of a down draught. It may be confirmed that the hydrodynamic equations in Boussinesq approximation given above satisfy this symmetry.

B. Fourier Expansion

In view of the Boussinesq symmetry and the facts that $\cos(qa_x(L_x - x)) = (-1)^q \cos(qa_x x)$ and $\cos(pa_y(L_y - y)) = (-1)^p \cos(pa_y y)$, one sees that $T_{qp}(z)$ must be an odd function of z if $q + p$ is even, and it must be an even function of z if $q + p$ is odd. Since $T(x, y, \pm 1/2) = 0$, and since $\sin(2n\pi z)$ and $\cos((2n+1)\pi z)$ vanish at $z = \pm 1/2$, the expansion for the temperature is

$$\begin{aligned} T(\mathbf{r}) &= \sum_{q=0}^Q \sum_{p=0}^P \sum_{n=0}^N T_{qp n} \cos qa_x x \cos pa_y y \\ &\quad \times \begin{cases} \sin 2n\pi z, & q + p \text{ even}, \\ \cos 2n'\pi z, & q + p \text{ odd}, \end{cases} \end{aligned} \quad (6.86)$$

where $n' \equiv (2n+1)/2$, and $T_{qp0} = 0$ if $q + p$ is even. The vertical component of velocity has a similar expansion

$$\begin{aligned} v_z(\mathbf{r}) &= \sum_{q=0}^Q \sum_{p=0}^P \sum_{n=0}^N v_{qp n}^z \cos qa_x x \cos pa_y y \\ &\quad \times \begin{cases} \sin 2n\pi z, & q + p \text{ even}, \\ \cos 2n'\pi z, & q + p \text{ odd}. \end{cases} \end{aligned} \quad (6.87)$$

The x component of velocity has the expansion

$$\begin{aligned} v_x(\mathbf{r}) &= \sum_{q=0}^Q \sum_{p=0}^P \sum_{n=0}^N v_{qp n}^x \sin qa_x x \cos pa_y y \\ &\quad \times \begin{cases} \cos 2n'\pi z, & q + p \text{ even}, \\ \sin 2n\pi z, & q + p \text{ odd}, \end{cases} \end{aligned} \quad (6.88)$$

with $v_{0pn}^x = 0$. Similarly

$$\begin{aligned} v_y(\mathbf{r}) &= \sum_{q=0}^Q \sum_{p=0}^P \sum_{n=0}^N v_{qp n}^y \cos qa_x x \sin pa_y y \\ &\quad \times \begin{cases} \cos 2n'\pi z, & q + p \text{ even}, \\ \sin 2n\pi z, & q + p \text{ odd}, \end{cases} \end{aligned} \quad (6.89)$$

with $v_{q0n}^y = 0$. These latter two expansions arise from the Boussinesq symmetry and the vanishing of the velocity at $z = \pm 1/2$.

1. z -Component of the Velocity

Inserting the expansions for the temperature and the z -component of the velocity into Eq. (6.80) and setting the coefficients of each term to zero gives the particular solution

$$v_{qp}^{zp} = \frac{\mathcal{R}[(qa_x)^2 + (pa_y)^2]}{[(qa_x)^2 + (pa_y)^2 + \mathcal{M}_n^2]^2} T_{qp} \quad (6.90)$$

where

$$\mathcal{M}_n \equiv \begin{cases} 2n\pi, & q+p \text{ even}, \\ (2n+1)\pi, & q+p \text{ odd}. \end{cases} \quad (6.91)$$

Note the distinction between the superscript p , for particular, and the subscript p , an integer index.

The homogeneous solution satisfies $\nabla^2 \nabla^2 v_z^h(\mathbf{r}) = 0$. It has the expansion

$$v_z^h(\mathbf{r}) = \sum_{q=0}^Q \sum_{p=0}^P \cos qa_x x \cos pa_y y \times \begin{cases} f_{qp}^{zs}(z), & q+p \text{ even}, \\ f_{qp}^{zc}(z), & q+p \text{ odd}. \end{cases} \quad (6.92)$$

Here it may be readily verified that the odd homogeneous solution is

$$f_{qp}^{zs}(z) = A_{qp} \sinh(\alpha_{qp} z) + B_{qp} z \cosh(\alpha_{qp} z), \quad (6.93)$$

and that the even homogeneous solution is

$$f_{qp}^{zc}(z) = A_{qp} \cosh(\alpha_{qp} z) + B_{qp} z \sinh(\alpha_{qp} z), \quad (6.94)$$

with

$$\alpha_{qp} = \sqrt{(qa_x)^2 + (pa_y)^2}. \quad (6.95)$$

Even and odd in this context refer to the parity with respect to z .

With $v_z(\mathbf{r}) = v_z^p(\mathbf{r}) + v_z^h(\mathbf{r})$, the four boundary conditions, $v_z(x, y, \pm 1/2) = 0$ and $\partial v_z(x, y, z)/\partial z|_{z=\pm 1/2} = 0$, determine the coefficients A_{qp} and B_{qp} in the even and odd cases. It is straightforward to use the orthogonality properties of the trigonometric functions to obtain the Fourier coefficients, v_{qp}^z .

2. x - and y -Components of the Velocity

The lateral components of the velocity can be written in the form

$$v_x(\mathbf{r}) = \sum_{q=0}^Q \sum_{p=0}^P f_{qp}^x(z) \sin qa_x x \cos pa_y y, \quad (6.96)$$

and

$$v_y(\mathbf{r}) = \sum_{q=0}^Q \sum_{p=0}^P f_{qp}^y(z) \cos qa_x x \sin pa_y y. \quad (6.97)$$

In view of Eqs (6.78) and (6.79), one has

$$f_{qp}^x(z) = qa_x f_{qp}(z), \text{ and } f_{qp}^y(z) = pa_y f_{qp}(z). \quad (6.98)$$

Inserting these into the density equation, $\nabla \cdot \mathbf{v}(\mathbf{r}) = 0$, and equating the lateral coefficients term by term yields

$$f_{qp}(z) = \frac{1}{(qa_x)^2 + (pa_y)^2} \sum_{n=1}^N v_{qp}^z \times \begin{cases} (-2n\pi) \cos(2n\pi z), & q+p \text{ even}, \\ (2n'\pi) \sin(2n'\pi z), & q+p \text{ odd}. \end{cases} \quad (6.99)$$

The boundary condition $\mathbf{v}(x, y, \pm 1/2) = \mathbf{0}$ is automatically satisfied, having already been invoked in the solution of the z -component of the velocity. These solutions for the horizontal velocity can now be projected onto the original z -expansions, Eq. (6.88) and Eq. (6.89).

C. Algorithm

This cross roll algorithm was used to model the cross roll transition from a steady straight roll state with wave number a_y to an orthogonal straight roll state with wave number \bar{a}_x . As in the first form of the ideal straight roll algorithm described in §VD 1, a_y was fixed typically in the neutrally stable range $\approx [2, 10]$, with $P = 6$ and $N = 6$. (The P used here replaces the L used there.) This gave an adequate description of the straight rolls in comparison with the benchmark $L = N = 10$ calculations reported there. A small x -wave number, $a_x \approx 0.1$ – 0.5 , and a large number of modes, $Q \approx 60$ – 150 were used.

For the initial state, a steady straight roll state of wave number a_y generated by the first algorithm was used. In most cases, the value chosen for the initial wave number lay toward one of the extremities of the range of neutrally stable wave numbers for the Rayleigh number in the expectation of a transition to an intermediate wave number. The steady state temperature field was perturbed by adding an independent random number to each T_{qp} (white noise). The amplitude of the noise was proportional to the square root of the total power in the initial steady state. Typically, following the addition of the perturbation, the total power in the y -modes increased by about 10%, and the total power in the x -modes was twice as great as that in the y -modes, with ≈ 15 times as many x -modes as y -modes. A cross roll transition usually occurred to ideal straight rolls in the x -direction, with $\bar{a}_x = (2\bar{q} + 1)a_x \approx 3$ – 4.5 . Simple time stepping was used to obtain the evolution of the temperature field. The modal power, the sub-system entropy, and the reservoir entropy were monitored during the transition.

In some cases the computational burden was reduced by only allowing fundamental modes within a window about the likely outcome. That is, the temperature and velocity coefficients were set to zero unless they corresponded to an integer multiple (including zero) of a wave number within the window. Typically, a window

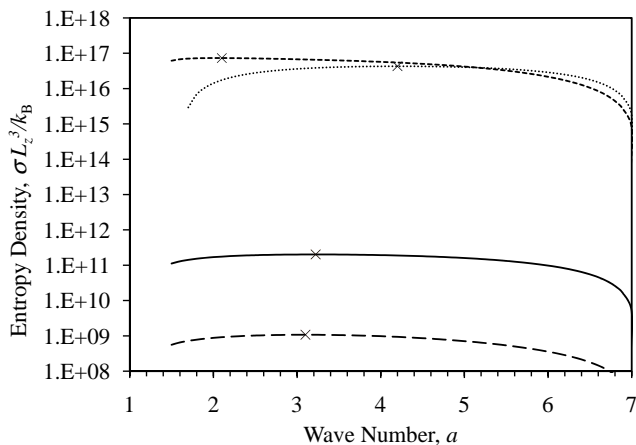


FIG. 1: Components of the convective entropy density (log scale) at $\mathcal{R} = 5000$. The solid curve is the gravitational contribution, Eq. (4.59), the long dashed curve is the negative of the kinetic energy contribution, Eq. (4.60), and the short dashed curve is the negative of the internal energy contribution, Eq. (4.58). The dotted curve is the sub-system entropy, Eq. (4.51). The crosses mark the maximum of each curve.

1–2 wave numbers wide halved the number of possible Fourier modes, and reduced the computer time by almost an order of magnitude. Tests with and without the window showed that it had little or no effect on the computed transitions. For example, at a Rayleigh number of $\mathcal{R} = 5000$, and for an initial wave number of $a_y = 4.3$, the average final wave number following the cross roll transition was $\langle \bar{a}_x \rangle = 3.32 \pm 0.05$ using a wave number step of $a_x = 0.15$ and no window, it was $\langle \bar{a}_x \rangle = 3.32 \pm 0.06$ with $a_x = 0.16$ and a window $[2.5, 4.5]$, and it was $\langle \bar{a}_x \rangle = 3.21 \pm 0.04$ with $a_x = 0.11$ and a window $[2.9, 4.0]$. The standard deviation of the transitions appeared to depend upon the wave number step, with it being larger than or equal to the wave number step.

These equations for cross roll convection and their computational implementation have been tested by setting $Q = 0$ and comparing the steady state results with those obtained with the independent straight roll program.

VII. CONVECTION THEORY AND EXPERIMENT

In this section the results of the convection calculations are presented using the material properties for a typical silicone oil with $\nu = 0.1$.^{31,32} Figure 1 shows the three contributions to the convective entropy density at $\mathcal{R} = 5000$. This is the difference in entropy between convection and conduction calculated using the static part of the reservoir entropy, as described in §IV. The figure also shows the sub-system entropy density (i.e. the difference in the sub-system entropy between the convecting state and the conducting state). All of the wave numbers

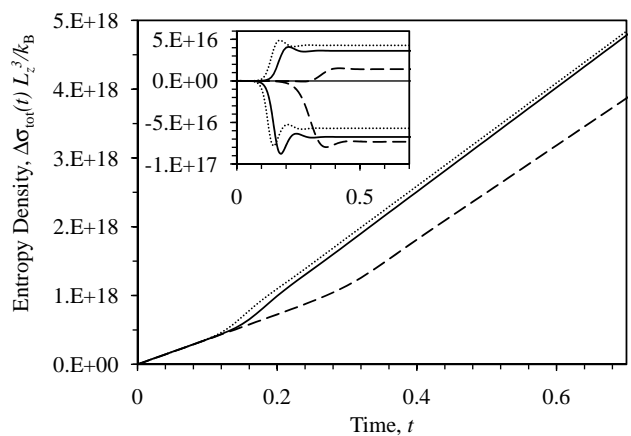


FIG. 2: Change in entropy density during a spontaneous straight roll transition from conduction at $\mathcal{R} = 5000$. The solid curves are for $a = 3$, the dashed curves are for $a = 2$, and the dotted curves are for $a = 4$. In the main figure, the curves are the change in the total entropy density, Eq. (4.63). In the inset, the lower three curves are the internal entropy part of the static convection entropy, Eq. (4.58), the upper three curves are the sub-system entropy, Eq. (4.51), and the horizontal line is a guide to the eye.

in this and the following figures correspond to hydrodynamic steady states, with the low wave number end of the curves signifying the limit to the steady state ideal straight roll solutions to the Boussinesq equations. These are the so-called neutrally stable states for which steady state straight roll solutions exist. The central region of the neutrally stable region is absolutely stable, (i.e. perturbations decay and the original straight roll state remains). The extreme wave numbers toward the boundaries of the neutrally stable region are generally unstable to perturbations, which result in either a new straight roll state with a different wave number, as might occur via the zig-zag or cross roll transition, or else another type of convective pattern.

It can be seen that the entropy due to the convective temperature field itself, the internal energy contribution Eq. (4.58), is about six orders of magnitude greater than the entropy directly due to gravity, which in turn is about two orders of magnitude greater than the entropy due to the kinetic energy. These results are typical for the whole range of Rayleigh numbers. Hence due to this dominance it makes no difference whether one discusses the full static form of the convective entropy or just the internal energy contribution. The sub-system entropy itself, Eq. (4.51), is comparable in magnitude to the static convective entropy, but it is positive. It decreases in magnitude approaching the limits of the range of steady state solutions and actually becomes negative at the low wave number end in most cases.

The static convective entropy difference, which, as shown in Fig. 1, is dominated by the internal energy, is negative. One should *not* conclude from this that the convecting state is thermodynamically unfavorable,

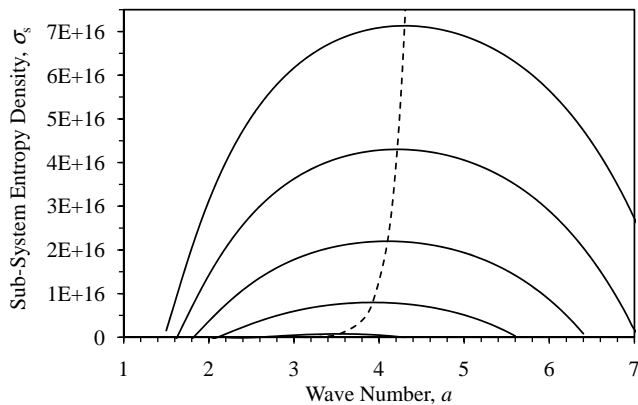


FIG. 3: Sub-system entropy density for ideal straight roll convection for wave numbers in the region of neutral stability, for Rayleigh numbers from 2000 (bottom) to 6000 (top), in steps of 1000. The dashed curve shows the maxima.

since this would contradict the hydrodynamic calculations, which show that the convecting states are stable and arise spontaneously from the conducting state with an initial perturbation. It can be seen in Fig. 2 that the change in the total entropy density, Eq. (4.63), during a straight roll transition is positive. This contrasts with the static part of the entropy difference, Eq. (4.58), which is negative throughout the transition. The difference in the sub-system entropy, Eq. (4.51), is mainly positive, but not during the entire transition. (The initial data for $a = 2$ in the inset, which can only just be resolved on the scale of the figure, is negative.) The slope of the change in total entropy density is the dissipation (the rate of entropy production of the reservoirs), which is proportional to the Nusselt number for each case. It can be seen that it is constant at longer times as the sub-system achieves its final structure. The entropy change of the reservoirs completely dominates the change in entropy of the total system during the transition. It is always found that the change in the total entropy density is positive at each stage of the conduction-convection transition. This means that there is indeed consistency between hydrodynamic stability and the Second Law of Thermodynamics.

Figure 3 shows the difference in the sub-system entropy between convection and conduction, Eq. (4.51), for ideal straight rolls as a function of wave number for several Rayleigh numbers. Steady state straight roll solutions could be obtained in the range $1708 \leq \mathcal{R} \lesssim 55,000$, with the range of neutral stability increasing with increasing Rayleigh number (at least initially). It can be seen that at a given wave number, the sub-system entropy density increases with increasing Rayleigh number, and that it approaches zero toward the ends of the stable range. The linear stability analysis of the hydrodynamic equations predicts that the convective transition occurs at $\mathcal{R}_c = 1708$ and $a_c = 3.117$.^{25,26} As the critical Rayleigh number is approached from above along the critical wave number, the sub-system entropy density approaches zero

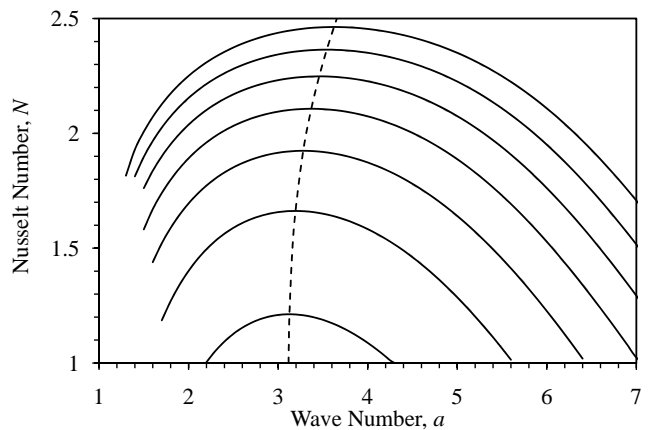


FIG. 4: Nusselt number as a function of wave number, for Rayleigh numbers from 2000 (bottom) to 8000 (top), in steps of 1000. The maxima are shown by the dashed curve.

from above. Apart from the low wave number end of the steady state range, the change in sub-system entropy density from conduction was found to be positive. As mentioned in connection with Fig. 2, the sub-system entropy density was not always positive during the approach to the steady state, and it was also negative in many stable states toward the low wave number end of the range.

It can be seen in Fig. 3 that the first and the second derivatives of the sub-system convective entropy density vanish at the critical wave number and critical Rayleigh number. This is analogous to behaviour in equilibrium systems where entropy derivatives vanish at the critical point. In convection, it is known that the hydrodynamic fluctuations diverge at the convective instability (see Ref. 33 and references therein). The precise meaning of the vanishing of the sub-system entropy derivatives at the critical point and the connection with divergent hydrodynamic fluctuations is not clear to the present author.

Figure 4 shows the Nusselt number for various Rayleigh numbers as a function of wave number over the region of neutral stability. As in the preceding figures, the curves represent steady state straight roll convection. There is a well-defined wave number of maximum heat flux at each Rayleigh number, and this increases with increasing Rayleigh number.

The significance of this figure relates to the discussion in §II regarding the Principles of Maximum and Minimum Dissipation, which assert respectively that the optimum non-equilibrium state is determined by either the greatest or else the least rate of entropy production. Since the dissipation is linearly proportional to the Nusselt number, if one or other of these principles were true, then the optimum wave number for straight roll convection at each Rayleigh number could be read directly from Fig. 4. It can be seen that the wave number of minimum dissipation occurs at the large wave number boundary

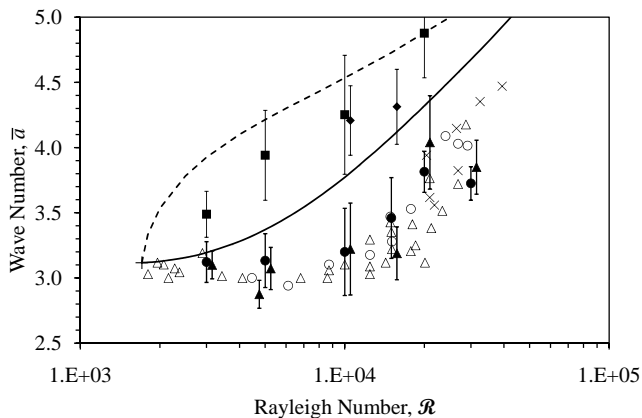


FIG. 5: The ideal straight roll wave number following a spontaneous transition as a function of Rayleigh number (log scale). The open symbols are measured cross roll transitions³⁴ and the closed circles and triangles are cross roll calculations ($P = N = 6$, $Q = 100$ – 150 , $a_x = 0.1$ – 0.2 , error bars give the standard deviation, with the data shifted horizontally by $\pm 5\%$). The initial constrained state had a large wave number (triangles), a medium wave number (crosses), or a small wave number (circles). The closed squares ($L = 100$ and $a_y = 0.2$) and closed diamonds ($L = 150$ and $a_y = 0.1$) are the calculated wave number following a conduction–convection transition. The curves give the calculated wave number of maximum Nusselt number (solid curve) and of maximum sub-system entropy density, Eq. (4.51), (dashed curve).

of the neutrally stable range, and that the wave number of maximum dissipation is near the critical wave number and increases with increasing Rayleigh number.

Fig. 5 compares several results for the wave number of ideal straight roll convection: those that result from spontaneous cross roll transitions, both experimentally measured³⁴ and the present calculations, those calculated for a direct transition from conduction, and those calculated to give the maximum Nusselt number and the maximum sub-system entropy.

The experimentally measured wave numbers are taken from Fig. 7 of Ref. 34. The experiments were performed by initially constraining the system in a straight roll convecting state with a wave number specified by means of a periodic temperature perturbation (obtained with an intense light source and shadow mask). Upon removal of the perturbation, there often occurred a spontaneous transition via an intermediate cross roll state to an orthogonal straight roll state whose wave number is shown in Fig. 5. Only final states that resulted from a cross roll transition and that are entirely or predominantly straight rolls are analysed here. Spontaneous zig-zag transitions to straight roll states, also occurred but these are not included in the figure. The majority of the measurements of Busse and Whitehead³⁴ either did not result in a spontaneous transition, or else did not have a final straight roll state, or else had too many defects; none of these were analysed. The measurements of Chen and Whitehead,³⁵ did result in ideal straight rolls, but the data was prob-

lematic because they were obtained in a cylindrical cell and because only the range of final wave numbers rather than the individual transitions was reported. Almost all other measurements in the literature of the convective wavelength could not be analysed for similar reasons: either no spontaneous transition occurred, or else the initial state was not a straight roll state, or else the final state was not a straight roll state, or else there were many defects in the final state.^{36–42}

It can be mentioned in passing that the measured wave numbers³⁴ increase with increasing Rayleigh number, as can be seen in Fig. 5. Most measurements on convection reported in the literature show the opposite trend (see Refs. 43–48 and also references in Ref. 49). The reason for the difference is that most measurements are for curved convection rolls, due either to using a cylindrical cell, or else to the presence of point defects, and for these the hydrodynamic equations fix the steady state solutions to have a wave number that decreases with increasing Rayleigh number.^{50–53}

Busse and Whitehead³⁴ classified the initial wave number as small, medium, or large, as indicated by the symbols in Fig. 5. The experimental measurements indicate that the wave number can both increase and decrease in a spontaneous transition, depending upon the initial constrained wave number and Rayleigh number. It is difficult to see a systematic dependence on the initial wave number in the measured experimental data (but see Fig. 8 below). The measurements (and calculations) show that there are barriers to changing the straight roll wave number since continuous evolution of the wave number was not observed, and once the orthogonal wave number is established in the intermediate cross roll state, it remains as the wave number of the final straight roll state. Consistent with the calculations, there is a certain width or scatter in the measured final wave number at each Rayleigh number, which suggests that it depends upon the initial wave number, and also that it depends upon the initial state or the actual destabilising perturbation.

The experimental data is compared in Fig. 5 with the calculated wave numbers that give the maximum heat flux and the maximum sub-system convective entropy at each Rayleigh number. There is no real agreement between the observed final wave numbers and the wave number that maximises the heat flux or the sub-system entropy. There is some similarity in the observed and calculated wave numbers in that they tend to increase with increasing Rayleigh number. This similarity is no more than qualitative. These data provide evidence that neither the heat flux nor the sub-system entropy is maximised in the non-equilibrium state. Since the static part of the entropy difference is negative, one can also conclude that it does not determine the non-equilibrium state.

Results for the final wave number $\langle \bar{a}_x \rangle$ of the cross roll transition algorithm described in §VIC are also shown in Fig. 5. These use $Q = 100$ and $a_x = 0.2$, or $Q = 150$

and $a_x = 0.1$. Both small, $a_y = 2.2$ – 2.4 , and large, $a_y = 4.3$ – 6.0 , wave number initial states were used, with white noise added as an initial perturbation. The number of independent trials for each initial wave number was 5–13. The bars in the figure signify the standard deviation of the transition rather than the standard error of the average final wave number. In some cases the standard deviation was observed to depend on the wave number step used in the calculations; it was generally not less than the wave number step. Each calculation was terminated when it was judged that no further transition would occur, generally on the basis that the power in the maximal x -mode was clearly dominant. The logarithm of the number of transitions observed from a given initial wave number to a given final wave number is directly related to the second entropy of the transition. It can be seen in Fig. 5 that there is quantitative agreement between the calculated and measured final wave numbers. This provides additional confirmation of both the cross roll computer program and algorithm and also of the applicability of the hydrodynamic model to the experimental system.

It ought be mentioned that there is the possibility of bias in the statistics in the present computations due to the judgement that has to be exercised in deciding that a transition to an ideal straight roll state has occurred. For example, for the case of a Rayleigh number of $\mathcal{R} = 5000$ and an initial wave number of $a_y = 6.2$, 16 trials were run. Of these, 7 had a clear transition to an ideal straight roll state by times $t < 4$, with an average final wave number $\langle \bar{a}_x \rangle = 3.01 \pm .04$. The remaining 9 trials exhibited Bloch states, in which two or more neighboring wave numbers were dominant with comparable power, and which were evolving exceedingly slowly. Five of these Bloch states were terminated at times $t < 4$ and discarded. The remaining 4 were run until $t = 11$ – 13 , with 3 ending up in a clear ideal straight roll state, with $\langle \bar{a}_x \rangle = 2.77 \pm .07$, and the remaining 1 being terminated at $t = 10.9$ without a clear result (although it appeared to be converging toward $\bar{a}_x = 2.9$). If one had retained only trials with a clear transition by $t = 4$, then one would have obtained $\langle \bar{a}_x \rangle = 3.01 \pm .04$. If one simply averaged over all transitions that had actually been completed, then the average is $\langle \bar{a}_x \rangle = 2.94 \pm .05$. But this last result is biased because slowly evolving cases are the ones discarded and these would have had a smaller wave number if they had been allowed to go to completion. If one removed this bias by weighting the short and long time averages in the ratio 7:9 (i.e. according to the number of Bloch states), then the average is $\langle \bar{a}_x \rangle = 2.88 \pm .04$. In summary, in this case ($\mathcal{R} = 5000$, $a_y = 6.2$) rapid transitions had a larger final wave number than transitions that took more time. Only a small minority of all the cases run were terminated without a result, and so it is likely that this potential bias does not have a significant effect on the computational results in Fig. 5. Whether or not it is a potential experimental problem is unclear.

In addition to the cross roll transition, Fig. 5 also

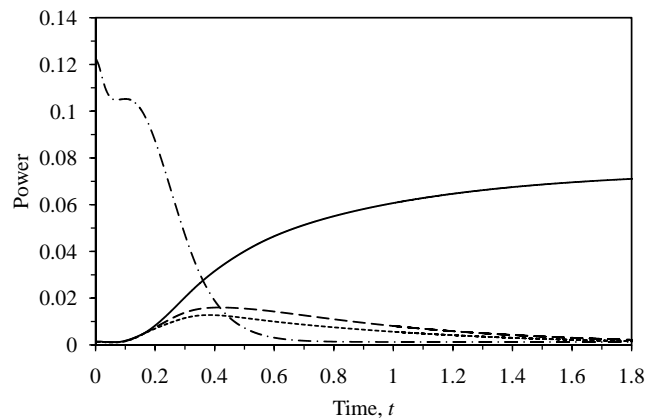


FIG. 6: The calculated modal power during a cross roll transition ($\mathcal{R} = 5000$, $a_y = 1.7$, $\bar{a}_x = 3.41$, $a_x = 0.31$, $Q = 80$, and $P = N = 6$). The solid, dashed, and dotted curves are the three x -modes with highest power, and the dash-dotted curve is the total power in the y -modes.

shows the average final wave number for the conduction–convection transition, $\langle \bar{a}_y \rangle$, whose calculation was described in §VD 2. White noise was used as a perturbation to initiate the transition. The average final wave number appeared insensitive to the wave number step ($a_y = 0.1$ or 0.2), although the standard deviation was smaller for the smaller step. It was found that in most cases the system converged to a straight roll steady state that was an odd harmonic of the small wave number, $\bar{a} = (2\bar{l} + 1)a$, as demanded by the Boussinesq symmetry. Beyond $\mathcal{R} \gtrsim 20,000$, ideal straight rolls did not result, or at least there was not a single clearly dominant wave number. (Some such Bloch states are included in the averages for $\mathcal{R} = 15,000$ in Fig. 5.) It can be seen that the wave number resulting from the direct conduction–convection transition is larger than that resulting from a cross roll transition.

These results show that the two types of phase transition, conduction–convection and cross roll, differ significantly even though both result in the same type of final state, namely ideal straight rolls. At a given Rayleigh number, the ideal straight roll wave number depends upon whether it results directly from conduction, or whether it results from a cross roll transition (and, in the latter case, it depends on the initial wave number, as shown in Fig. 8 below). One can conclude from this that a single time variational quantity whose optimisation determines the favored non-equilibrium pattern either does not exist, or else has negligible influence compared to the barriers between the multiple possible patterns. This is likely to be a general feature of non-equilibrium systems, and instead of seeking ‘the’ optimum pattern or phase, one should focus on the optimum transition from a given phase.

The transition between two orthogonal straight roll convective states via the cross roll intermediate state, as

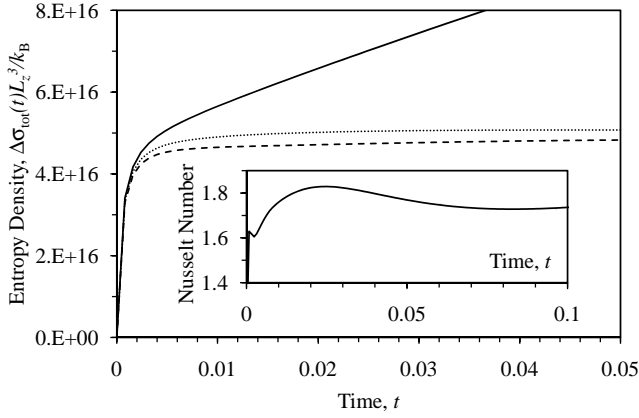


FIG. 7: Change in entropy density during the cross roll transition of the preceding figure. The solid curve is the change in total entropy density, Eq. (4.63), the dashed curve is the change in the internal entropy part of the static convection entropy, Eq. (4.58), and the dotted curve is the change in the sub-system entropy, Eq. (4.51). The inset shows the Nusselt number.

described in §VI, can be monitored by the evolution of the power in the various modes, as shown in Fig. 6. In this case the system was initially in a convecting straight roll steady state with $a_y = 1.7$, near the lower end of stable states, and at $t = 0$ white noise was added to all the modes. This increased the total power in the y -modes by about 10%, and created almost twice as much power in the x -modes as in the y -modes, spread over thirteen times as many modes. The power in the x -mode q was defined as $P_{xq} \equiv \sum_n T_{q0n}^2$, and the total power in the x -modes was defined as $P_x \equiv \sum_q P_{xq}$, and similarly for the y -modes.

The initial white noise perturbation is meant to model the experimental situation, although the origin of the noise is unclear. It is possible that noise originates from mechanical vibrations or from temperature inhomogeneities and water flow in the heat baths, in which cases white noise would likely be appropriate. Although the perturbation is small on the scale of the convective temperature, it is large on molecular scales, and so treating it as a thermodynamic fluctuation (i.e. weighting it by the exponential of the entropy) would be problematic.

Figure 6 shows that the power in the x -modes grows over time at the expense of the initially stable y -modes. By about $t \approx 0.6$ the y -rolls have disappeared, and by about $t \approx 1.5$ a steady straight roll convecting state has been established with $\bar{a}_x = 3.41 = 11 \times 0.31$. The Nusselt number at $t = 1.88$ was $\mathcal{N} = 2.110$, which compares well with $\mathcal{N} = 2.107$ calculated using the ideal straight roll algorithm of §V for $\mathcal{R} = 5000$ and $a = 3.4$. It can be concluded from the figure that a cross roll transition from one straight roll state to another has occurred. It may be called spontaneous in the sense that no constraint was imposed on the final state (other than that it be an odd

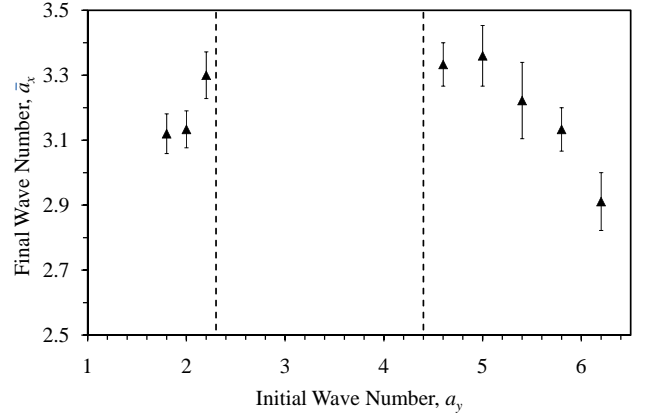


FIG. 8: The calculated final wave number \bar{a}_x as a function of the initial wave number a_y for cross roll transitions at $\mathcal{R} = 10,000$ ($Q = N = 6$, $P = 100$, and $a_x = 0.2$). The symbols signify the most likely final wave number averaged over 6–12 trials, and the vertical bars show the standard error on the mean. The vertical dashed lines bound the region of stable wave numbers for which no transition occurred.

integer multiple of the wave number step) or indeed on whether any transition would occur at all.

Figure 7 shows the evolution of the total entropy during a cross roll transition. It can be seen that the total entropy monotonically increases in time. It can also be seen that the change in the static part of the convective entropy and the change in the sub-system entropy are positive during the transition. The dissipation, which is the rate of change of the reservoir entropy, is proportional to the Nusselt number. Although the Nusselt number is higher for the final state than for the initial state, it can be seen from the inset that it does not increase monotonically during the transition. Since the proposition that the dissipation is maximised in the optimum non-equilibrium state implies that the dissipation increases during all stages of a spontaneous transition, the data in the inset provides further evidence against the maximum dissipation idea.

Figure 8 shows the final wave numbers calculated from a series of cross roll transitions for different initial wave numbers at a Rayleigh number of 10,000. Since only cross roll transitions were permitted in the computations, it is possible that the calculated cross roll domain is larger than the measured one because unlike the calculations, in the experiments other transitions can supersede the cross roll transitions. The most likely final wave number for any one trial is the wave number that, out of all possible wave numbers la_x , has the most power after a transition has occurred, $\bar{a}_x = (2\bar{l} + 1)a_x$. This varies between trials, and it is the average of these that is plotted for each initial wave number. It can be seen that the final wave number depends upon the initial wave number. One aspect of this dependence is the existence of a region of stable initial wave numbers for which no transition was observed (6 wave numbers spanning this region were tested, with

4–12 trials in each case). A second aspect is the systematic increase in final wave number with decreasing initial wave number for large initial wave numbers. One can possibly make out the opposite trend for small initial wave numbers. This variation of the final wave number is statistically significant. It is possible that at least part of the scatter of the experimental data³⁴ in Fig. 5 can be attributed to a similar dependence on the initial wave number. Also, the relatively small change in final wave number, as well as the opposite trend on either side of the stable region, are consistent with the experimental data³⁴ in Fig. 5 that appear to show no difference in the final wave number for systems that were in a small or in a large wave number initial state.

Another example of this dependence of the final state on the initial state is the zig-zag transition. Although not explored here, it is observed experimentally³⁴ that ideal straight rolls initially close to the low wave number neutrally stable boundary, a_i , can undergo a spontaneous zig-zag transition to another ideal straight roll state, oriented at 45° to the initial rolls, with final wave number $a_f = a_i\sqrt{2}$. Obviously then this is a clear example when, at a given Rayleigh number, the final state depends upon the initial state. Again the final state is determined by the thermodynamics of the transition itself rather than by any single time thermodynamic variational principle of the final state of ideal straight rolls.

Figure 8 brings the focus to the transitions rather than the states. For a given Rayleigh number and initial wave number, distinct final states (i.e. distinct transitions) occur with non-negligible probability (not shown). For example, in the case of $\mathcal{R} = 10,000$ and $a_y = 5.4$, 4 distinct transitions actually occurred in 9 trials, ($\bar{a}_x = 3.4$ occurred 4 times, $\bar{a}_x = 3.0$ occurred 3 times, $\bar{a}_x = 2.6$ occurred once, and $\bar{a}_x = 3.8$ occurred once). The existence of distinct final states from which no further transitions occur signifies that patterns with a given wave number are locally stable and that there are barriers to further transitions, which is consistent with the experimental observations.

The data in Fig. 8 imply that at a given Rayleigh number, it is less meaningful to speak of the average wave number for ideal straight roll convection than it is to speak of the average wave number following a transition from a given steady state. This particular point was already made in connection with Fig. 5, where the distinction between the wave number resulting from a conduction–convection transition and from a cross roll transition was discussed. Even this is a severe simplification of the full convective transition phenomenon, since the final wave number of the cross roll transition depends upon the initial wave number.

VIII. CONCLUSION

1. The Second Law of Thermodynamics

For an equilibrium system, the Second Law of Thermodynamics provides the variational principle that determines the optimum state. The primary statement of the law is that the total entropy increases during a spontaneous transition. The corollary of this is that the total entropy is maximised in the optimum state. (This is the same as minimising the free energy, which is minus the temperature times the total entropy.)²⁷

The Second Law of Thermodynamics rests on two distinct bases. First is quantitative evidence, originally experimental measurement, and, in more recent times, computational data. Second, is reason, namely Boltzmann’s identification of entropy with the logarithm of the molecular configurations that comprise a state. By linking entropy to probability, Boltzmann provided both an intuitive physical explanation of why entropy increases during spontaneous transitions, and also a mathematical prescription for calculating entropy and its evolution.

Just as important as what the Second Law says is what it does not say. Nothing quantitative is said about time. Implicitly the law gives the direction of time but not its speed. Specifically, the law says nothing about the rate of entropy increase, the dissipation.

There is a class of static systems, namely those that are hysteretic or metastable, that illuminate a specific aspect of the Second Law of Thermodynamics that is relevant to the discussion of heat flow that follows. Such systems include glasses and slowly relaxing substances, macromolecules, (e.g. the shape and conformation of proteins), and systems stuck beyond the usual phase transition point (i.e. absent nucleation sites). These systems can be quite stable (i.e. they do not change macroscopically over experimental time scales) and in this sense they can quite reasonably be described as equilibrium systems. And yet, the current state of such systems can depend upon their past history. As far as the Second Law of Thermodynamics is concerned, it is quite true that the total entropy has increased during the evolution of such systems to their current state. But the entropy is not necessarily a maximum in the current state. One interpretation of such systems is that they are trapped in a local entropy maximum (free energy minimum), and that there are barriers that prevent a transition to the state of global entropy maximum.

There are two relevant lessons that can be drawn from this example. The first is the importance of both evidence and reason for the Second Law of Thermodynamics. If the law were based only upon evidence, then the existence of such hysteretic or metastable systems would appear to invalidate it, or at least the corollary that the optimum state is the state of maximum entropy. However, because one has a reasonable physical interpretation of the Second Law, one can instead identify these cases as exceptions to the rule, and interpret them in

terms of barriers that preclude transition to the globally optimum state. The second lesson from this example is that entropy as a variational principle can have practical limitations in determining the actual state of the system.

2. Specific Conclusions for Heat Flow

Turning now to the specific results of this paper, one can draw some definite conclusions for convective heat flow. The Principle of Maximum or Minimum Dissipation was discussed in the introduction of the paper. This is the variational principle that some have postulated for non-equilibrium systems, namely that the optimum state is given by either a maximum or a minimum in the rate of entropy production. For the case of heat flow, the dissipation is the heat flux divided by the temperature gradient, which is essentially the Nusselt number. The results in Fig. 5 for a spontaneous cross roll transition show that neither the measured³⁴ nor the calculated final wave number correspond to the maximum Nusselt number. (The wave number of minimum Nusselt number would lie off the scale.) Similarly the calculated spontaneous conduction-convection transition yields a final state that does not correspond to an extremity of the Nusselt number. The present results, as well as earlier results,^{30,34} show that the observed convective patterns following a spontaneous transition do not correspond to either the maximum nor to the minimum heat flux. Hence the superficial conclusion from these quantitative observations is that neither the maximum dissipation nor the minimum dissipation yield the optimum non-equilibrium state.

It might be objected that one cannot draw this conclusion solely from the data because, as in the case of metastable or hysteretic equilibrium states, there are barriers that prevent transitions: a globally optimum state might still exist but it is simply not achieved in the experiments or calculations. In other words, the violation of the Principles of Extreme Dissipation might only be a matter of practice rather than of principle. Continuing the objection, even if barriers reduce the utility of the Principle in this system, one or other of the two Principles might still be valid, and it might be useful for other non-equilibrium systems.

There are two counter arguments to this objection. The first is quantitative and is illustrated in the inset of Fig. 7. There it is shown that the Nusselt number (equivalently, the heat flux or the dissipation) evolves non-monotonically during a spontaneous cross-roll transition. This rules out both Principles of Extreme Dissipation: the Nusselt number neither always increases nor always decreases during a spontaneous transition between convective states. Hence even if there were no barriers between different convective states, the optimum non-equilibrium state cannot correspond to an extremum of the Nusselt number.

The second counter argument is that neither of the

Principles of Extreme Dissipation is supported by reason. Unlike the Second Law of Thermodynamics, there is no molecular interpretation that provides a persuasive picture for maximal or minimal rates of entropy production. Hence there is no credible basis to argue that the results of these experiments and computations for convection are an exception to a general rule.

Besides ruling out any Principle of Extreme Dissipation for convective systems, the present calculations allow one to draw another quantitative conclusion for heat convection, namely that the final state of a spontaneous transition depends upon the initial state. This was shown in Fig. 5, where different straight roll states resulted, depending upon whether the initial state was the conducting state, or whether it was an orthogonal cross-roll state, and in Fig. 8, where it was shown that the final wave number for the cross roll transition varied with the initial wave number. A similar dependence is seen experimentally in the zig-zag transition.³⁴ These results imply that for heat convection a single time thermodynamic quantity (such as the heat flow, or the sub-system entropy, or the total system entropy) is practically insufficient to determine the optimum state following a spontaneous transition. The word ‘practically’ here recognises that it might be the barriers between convective states that give rise to the dependence on the initial state and so the insufficiency of a single time quantity might be one of practice rather than one of principle. (Just as the insufficiency of entropy for describing a metastable or hysteretic state is a limitation in practice that does not rule out entropy as an equilibrium principle.)

In summary, the present quantitative calculations for heat convection lead to two specific conclusions. First, the Nusselt number (equivalently, the heat flux or the dissipation) does not change monotonically during spontaneous transitions between convecting steady states. From this it follows that the Nusselt number cannot provide a variational principle for heat convection. And second, due to the presence of barriers signified by a dependence of the final state on the initial state, in practical terms there cannot be *any* single time variational principle for heat convection.

3. General Conclusions for Non-Equilibrium Systems

The behavior of the Nusselt number and its equivalence to the dissipation rules out any general principle for non-equilibrium systems that asserts that spontaneous transitions between states correspond to a monotonic change in the dissipation. The corollary of this is that there can be no general Principle of Extreme Dissipation for determining the optimum non-equilibrium state. (Non-equilibrium state means both flux and structure.) The mathematical basis for this general conclusion is just an axiom of Aristotelian logic: the single counter example of heat flow in convecting systems disproves the general theorem. The physical reason why there can be no principle

of extreme dissipation is outlined below.

Beyond the dissipation, general conclusion can be drawn about transitions. The specific results for heat convection obtained here shifts the focus from non-equilibrium states to the transitions between them. This was the conclusion drawn from Figs 5 and 8, namely that the observed non-equilibrium state is conditional upon the initial state prior to the transition. This highlights the importance of the second entropy as the variational principle for non-equilibrium systems, since it is the two-time thermodynamic quantity that gives the probability of transitions.

There are two reasons to believe that in general non-equilibrium systems are better characterised by their transitions than by their states. The first argument, which is no more than suggestive, is based on the observation that in general a non-equilibrium state often means a steady pattern that is defined by the contrast between distinct regions of fluxes and structure. It seems reasonable to conclude that each region must represent a locally stable state, and there must be barriers inhibiting transformation from one pattern to another. For the same reasons as in heat convection, in practice such barriers negate the efficacy of single time thermodynamic quantities compared with the transition entropy.

The second, more rigorous, reason is that the non-equilibrium systems of interest can generally be modeled as a thermodynamic gradient imposed on a sub-system by reservoirs, and it is the structure and flux of the sub-system that represents the non-equilibrium state being characterised. However, the thermodynamic gradient can also be considered as arising from a spontaneous fluctuation of the total system, with the consequent flux being the regression of that fluctuation. This means that the current state of the sub-system is really part of the end state of a transition from the initial fluctuation of the total system that occurred some time in the past. In ranking two alternative non-equilibrium states of the sub-system given the applied thermodynamic gradient, it is not valid to compare their structural entropies because one is not comparing two spontaneous fluctuations of the sub-system. Likewise, it is not valid to rank them according to their total entropies, again because the total entropy *now* is due not to a fluctuation *now*, but rather to a prior fluctuation of the total system. (If total entropy was the correct ordinal function, then the steady state with the greatest dissipation would always be the preferred state because it would have the greatest total

entropy after sufficiently long times. Hence the sentence immediately preceding these parenthetical remarks provides the physical reason for ruling out the Principle of Maximum Dissipation in general.) Instead of these one-time thermodynamic functions (the sub-system entropy, the total entropy, or the dissipation), one has to compare the two states conditioned on the fact that the fluctuation of the total system has already been regressing for some time. This is why two-time rather than one-time thermodynamic quantities provide the relevant variational principle for characterising the non-equilibrium state of the sub-system.

The regression of the total system obeys the Second Law of Thermodynamics, namely that the total entropy increases over time. Hence the total dissipation is positive for any non-equilibrium state. (For a steady state of the sub-system, the total dissipation equals the dissipation of the reservoirs.) In analysing the possibility of a transition from one steady state to another, the Second Law of Thermodynamics demands only that the total dissipation must continue to be positive. It does not say that the dissipation has to increase. Even if the entropy of the sub-system for the final state is lower than that for the initial state, the transition is permitted provided that the decrease in sub-system entropy is smaller in magnitude than the integral of the reservoir dissipation over the time interval of the transition. (In such cases, this sets an upper bound on the speed of the transition.)

The second entropy is essentially the logarithm of the number of molecular configurations that give the transition. Its exponential gives the probability of a transition from one non-equilibrium state to another. Hence the second entropy is the two-time thermodynamic quantity that characterises non-equilibrium states and patterns.

In the present paper the second entropy appeared in two, indirect, ways. First, the hydrodynamic equations are equivalent to maximising the second entropy with respect to the fluxes, whilst accounting for the material conservation laws and equilibrium equation of state (see Refs 54–57 and Ch. 5 of Ref. 12). Second, the accumulation of trial transitions between steady convecting states is equivalent to mapping out the second entropy conditioned on the initial state. These two applications of the second entropy demonstrate its utility. The specific results obtained here for heat convection support the general conclusion that the two-time second entropy (or its generalisations for non-Markov systems)¹² is the variational principle for non-equilibrium systems.

¹ E. T. Jaynes, *Ann. Rev. Phys. Chem.* **31**, 579 (1980).

² G. D. Kirchhoff, *Ann. Phys.* **75**, 189 (1848).

³ P. Županović, D. Juretić, and S. Botrić, *Phys. Rev. E* **70**, 056108 (2004).

⁴ L. Onsager, *Phys. Rev.* **37**, 405 (1931).

⁵ L. Onsager, *Phys. Rev.* **38**, 2265 (1931).

⁶ I. Prigogine, *‘Introduction to Thermodynamics of Irre-*

versible Processes’, (Interscience, New York, 1967).

⁷ S. R. de Groot and P. Mazur, *‘Non-equilibrium Thermodynamics’*, (Dover, New York, 1984).

⁸ L. Onsager, *‘The Motion of Ions: Principles and Concepts’*, (Nobel Lecture, Dec. 11, 1968).

⁹ P. Mazur, in *‘The Collected Works of Lars Onsager’*, P. C. Hemmer, H. Holden, and S. Kjelstrup Ratkje, (eds) (World

- Scientific, Singapore, 1996), p. 61.
- ¹⁰ J. W. S. Rayleigh, *Proc. Math. Soc. London* **4**, 357 (1873).
 - J. W. S. Rayleigh, 'Theory of Sound', (MacMillan Co., London, 1st ed., 1877), Vol. I, p. 102.
 - ¹¹ P. Attard, *J. Chem. Phys.* **122**, 154101 (2005).
 - ¹² P. Attard, 'Non-Equilibrium Thermodynamics and Statistical Mechanics: Foundations and Applications', (Oxford University Press, Oxford, 2012).
 - ¹³ P. Attard, *Entropy* **10**, 380 (2008).
 - ¹⁴ L. Onsager and S. Machlup, *Phys. Rev.* **91**, 1505 (1953).
 - ¹⁵ J. Keizer, 'Statistical Thermodynamics of Non-equilibrium Processes', (Springer-Verlag, New York, 1987).
 - ¹⁶ H. Haken, *Z. Phys. B* **24**, 321 (1976).
 - ¹⁷ R. Graham, *Z. Phys. B* **26**, 281 (1977).
 - ¹⁸ H. Grabert and M. S. Green, *Phys. Rev. A* **19**, 1747 (1979).
 - ¹⁹ K. L. C. Hunt and J. Ross, *J. Chem. Phys.* **75**, 976 (1981).
 - ²⁰ B. H. Lavenda, 'Nonequilibrium Statistical Thermodynamics', (Wiley, Chichester, 1985).
 - ²¹ G. L. Eyink, *J. Stat. Phys.* **61**, 533 (1990).
 - ²² B. Peng, K. L. C. Hunt, P. M. Hunt, A. Suarez, and J. Ross, *J. Chem. Phys.* **102**, 4548 (1995).
 - ²³ I. Gyarmati, *Zeitschrift Fur Physikalische Chemie-Leipzig* **239**, 133 (1968).
 - ²⁴ I. Gyarmati, 'Nonequilibrium Thermodynamics, Field Theory, and Variational Principles', (Springer, Berlin, 1970).
 - ²⁵ C.-S. Yih, 'Fluid Mechanics: A Concise Introduction', (West River Press, Ann Arbor, 1977).
 - ²⁶ P. G. Drazin and W. H. Reid, 'Hydrodynamic Stability', (Cambridge University Press, Cambridge, 1981).
 - ²⁷ P. Attard, 'Thermodynamics and Statistical Mechanics: Equilibrium by Entropy Maximisation', (Academic Press, London, 2002).
 - ²⁸ P. Attard, *J. Chem. Phys.* **124**, 224103 (2006).
 - ²⁹ P. Attard, *J. Chem. Phys.* **121**, 7076 (2004).
 - ³⁰ F. H. Busse, *J. Math. and Phys.* **46**, 140 (1967).
 - ³¹ M. Dubois and P. Bergé, *J. Fluid Mech.* **85**, 641 (1978).
 - ³² The physical parameters of the silicone oil are: temperature $T_{00} = 298$ K, density $\rho_{00} = 0.960$ g cm⁻³, kinematic viscosity $\nu = 1.056$ cm² s⁻¹, thermal expansivity $\alpha = 0.96 \times 10^{-3}$ K⁻¹, thermal conductivity $\lambda = 3.7 \times 10^{-4}$ cal cm⁻¹ K⁻¹ s⁻¹, specific heat $c_p^\dagger = 0.337$ cal g⁻¹ K⁻¹, and thermal diffusivity $\kappa = 1.14 \times 10^{-3}$ cm² s⁻¹. From line 1 of Table I of Ref. 31.
 - ³³ J. M. Ortiz de Zárate and J. V. Sengers, *Physica A* **300**, 25 (2001).
 - ³⁴ F. H. Busse and J. A. Whitehead, *J. Fluid Mech.* **47**, 305 (1971).
 - ³⁵ M. M. Chen and J. A. Whitehead, *J. Fluid. Mech.* **31**, 1 (1968).
 - ³⁶ R. J. Schmidt and O. A. Saunders, *Proc. Roy. Soc. A* **165**, 216 (1938).
 - ³⁷ J. W. Deardorff and G. E. Willis, *J. Fluid Mech.* **23**, 337 (1965).
 - ³⁸ E. L. Koschmieder, *Beit. Z. Phys. Atmos.* **39**, 1 (1966).
 - ³⁹ H. T. Rossby, *J. Fluid Mech.* **36**, 309 (1969).
 - ⁴⁰ R. Krishnamurti, *J. Fluid Mech.* **42**, 295 (1970).
 - ⁴¹ G. E. Willis, J. W. Deardorff, and R. C. J. Somerville, *J. Fluid Mech.* **54**, 351 (1972).
 - ⁴² E. L. Koschmieder and S. G. Pallas, *Int. J. Heat Mass Transfer* **17**, 991 (1974).
 - ⁴³ E. L. Koschmieder, *Adv. Chem. Phys.* **26**, 177 (1974).
 - ⁴⁴ C. Normand, Y. Pomeau, and M. G. Velarde, *Rev. Mod. Phys.* **49**, 581 (1977).
 - ⁴⁵ J. P. Gollub and A. R. McCarriar, *Phys. Rev. A* **26**, 3470 (1982).
 - ⁴⁶ P. Bergé and M. Dubois, *Contemp. Phys.* **25**, 535 (1984).
 - ⁴⁷ P. Kolodner, R. W. Walden, A. Passner, and C. M. Surko, *J. Fluid Mech.* **163**, 195 (1986).
 - ⁴⁸ M. Cross and H. S. Greenside, 'Pattern Formation and Dynamics in Non-equilibrium Systems', (Cambridge University Press, Cambridge, 2009).
 - ⁴⁹ A. V. Getling, 'Rayleigh-Bénard Convection: Structure and Dynamics', (World Scientific, Singapore, 1998).
 - ⁵⁰ Y. Pomeau and P. Manneville, *J. Phys. (Paris)* **42**, 1067 (1981).
 - ⁵¹ M. C. Cross, *Phys. Rev. A* **27**, 490 (1983).
 - ⁵² P. Manneville and J. M. Piquemal, *Phys. Rev. A* **28**, 1774 (1983).
 - ⁵³ J. C. Buell and I. Catton, *Phys. Fluids* **29**, 23 (1986).
 - ⁵⁴ L. D. Landau and E. M. Lifshitz, *Sov. Phys. JETP* **5**, 512 (1957).
 - ⁵⁵ L. D. Landau and E. M. Lifshitz, 'Fluid Mechanics', (Pergamon Press, Oxford, 1959).
 - ⁵⁶ J. M. Ortiz de Zárate, and J. V. Sengers, 'Hydrodynamic Fluctuations in Fluids and Fluid Mixtures', (Elsevier, Amsterdam, 2006).
 - ⁵⁷ P. Attard, *J. Chem. Phys.* **131**, 184509 (2009).